Journal of Medicinal Chemistry

Article

Specific correction of alternative survival motor neuron 2 (SMN2) splicing by small molecules: Discovery of a potential novel medicine to treat spinal muscular atrophy

Hasane Ratni, Gary M. Karp, Marla Weetall, Nikolai N. Naryshkin, Sergey V. Paushkin, Karen S. Chen, Kathleen D. McCarthy, Hongyan Qi, Anthony Turpoff, Matthew G Woll, Xiaoyan Zhang, Nanjing Zhang, Tianle Yang, Amal Dakka, Priya Vazirani, Xin Zhao, Emmanuel Pinard, Luke Green, Pascale David-Pierson, Dietrich Tuerck, Agnès Poirier, Wolfgang Muster, Stephan Kirchner, Lutz Mueller, Irene Gerlach, and Friedrich Metzger

J. Med. Chem., **Just Accepted Manuscript** • DOI: 10.1021/acs.jmedchem.6b00459 • Publication Date (Web): 14 Jun 2016

ACS Publications

Journal of Medicinal Chemistry is published by the American Chemical Society. 1155 Sixteenth Street N.W., Washington, DC 20036

Specific correction of alternative survival motor neuron 2 (SMN2) splicing by small molecules: Discovery of a potential novel medicine to treat spinal muscular atrophy

Hasane Ratni[1], Gary M. Karp[2]*, Marla Weetall[2], Nikolai A. Naryshkin[2], Sergey V. Paushkin[3], Karen S. Chen[3], Kathleen D. McCarthy[3], Hongyan Qi[2], Anthony Turpoff[2], Matthew G. Woll[2], Xiaoyan Zhang[2], Nanjing Zhang[2], Tianle Yang[2], Amal Dakka[2], Priya Vazirani[2], Xin Zhao[2], Emmanuel Pinard[1], Luke Green[1], Pascale David-Pierson[1], Dietrich Tuerck[1], Agnes Poirier[1],Wolfgang Muster[1], Stefan Kirchner[1], Lutz Mueller[1], Irene Gerlach[1], Friedrich Metzger[1]*

[1]F. Hoffmann-La Roche Ltd., pRED, Pharma Research & Early Development, Roche Innovation Center Basel, Grenzacherstrasse 124, 4070 Basel, Switzerland

[2]PTC Therapeutics, Inc., 100 Corporate Court, South Plainfield, NJ 07080, USA

[3]SMA Foundation, 888 Seventh Avenue, Suite 400, New York, NY 10019, USA

ABSTRACT

Spinal muscular atrophy (SMA) is the leading genetic cause of infant and toddler mortality, and there is currently no approved therapy available. SMA is caused by mutation or deletion of the survival motor neuron 1 (*SMN1*) gene. These mutations or deletions result in low levels of

functional SMN protein. *SMN2*, a paralogous gene to *SMN1*, undergoes alternative splicing and exclusion of exon 7, producing an unstable, truncated SMNΔ7 protein. Herein, we report the identification of pyrido-pyrimidinone series of small molecules that modify the alternative splicing of *SMN2*, increasing the production of full length *SMN2* mRNA. Upon oral administration of our small molecules, the levels of full length SMN protein were restored in two mouse models of SMA. In-depth lead optimization in the pyrido-pyrimidinone series culminated in the selection of compound **3** (RG7800), the first small molecule *SMN2* splicing modifier to enter human clinical trials.

INTRODUCTION

Spinal muscular atrophy (SMA) is the most common genetic cause of death of infants and toddlers with an incidence of 1 in 11,000 live births.[1] The disease varies in severity and presentation. There are three most common types of SMA. Patients with severe type I SMA can never sit and have a median survival around 2 years of age. Intermediately affected type II SMA patients can never stand unaided and commonly die in early adulthood. Those with the mildest form, type III SMA, have reduced motor function and may lose ambulation later in life.[2]

Survival motor neuron protein (SMN) is expressed in all body tissues, and is essential for normal development and functional homeostasis in all species.[3] Reduced levels of SMN protein result in loss of alpha motor neurons and progressive muscular atrophy. There is an inverse correlation between the quantity of full-length SMN protein expressed and disease severity.[4] In humans, SMN protein is produced by two paralogous genes: *SMN1* and *SMN2*. SMN protein expression is primarily driven by the *SMN1* gene. *SMN2* produces only low levels of full length mRNA due to alternative splicing of exon 7.

SMA results from a loss of function mutation or deletion of the *SMN1* gene, and the disease manifests by the insufficient generation of full length SMN protein by the *SMN2* gene. All SMA patients have at least one *SMN2* copy, and some may have up to six copies in a somatic cell.[4b] SMN protein levels generally correlate with *SMN2* copy number.[5] Relative to the levels of SMN in healthy individuals, SMN protein levels in SMA patients are reduced by approximately 70% in SMA type I, 50% in type II and 30% in type III.[4] This suggests that moderate increases in SMN protein levels can modify the disease severity. Therefore, our strategy to treat SMA has been to identify small molecules that shift the outcome of the alternative splicing of *SMN2* exon 7 towards the production of full length *SMN* mRNA and consequently functional SMN protein expression.

Over the last few years, a number of therapeutic options for SMA have been evaluated[5] and among them splicing correction of *SMN2* appears highly promising. It can be achieved either by intrathecal administration of antisense oligonucleotides (ASOs),[6] or advantageously by small molecules upon oral administration leading to both central and peripheral SMN protein increase as initially reported by us[7] and recently by others.[8]

We have reported the discovery of highly specific, orally available small molecules (coumarin **1**,[9] iso-coumarin **2**[10] and pyrido-pyrimidinone derivatives) that specifically modify *SMN2* splicing in SMA patient-derived cells and in two SMA mouse models, resulting in a clear therapeutic benefit in mice that model a severe SMA form.[7] However, the clinical development of the coumarin and iso-coumarin compounds **1** and **2** was mainly hampered by an in vitro flag in the Ames assay indicative of genotoxicity, phototoxicity, and chemical instability in plasma or aqueous buffers. These findings shifted our focus to the pyrido-pyimidinone series (Figure 1).

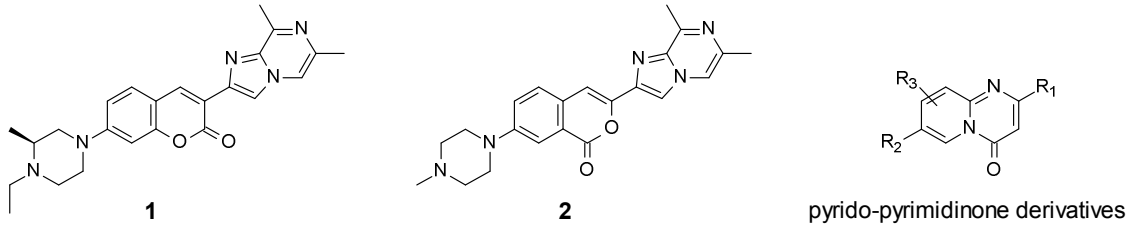

Figure 1. Coumarin **1**, iso-coumarin **2**, and pyrido-pyrimidinone derivatives.

We describe here the initial optimization attempts on the coumarin and iso-coumarin series, then we report the lead optimization strategy for the pyrido-pyrimidinone series addressing multiple issues that led to the discovery of orally active compounds **3-5** (Figure 2). Compound **3** was selected as our clinical candidate. It became the first orally active small molecule *SMN2* splicing modulator to enter human trials for the potential treatment of spinal muscular atrophy.

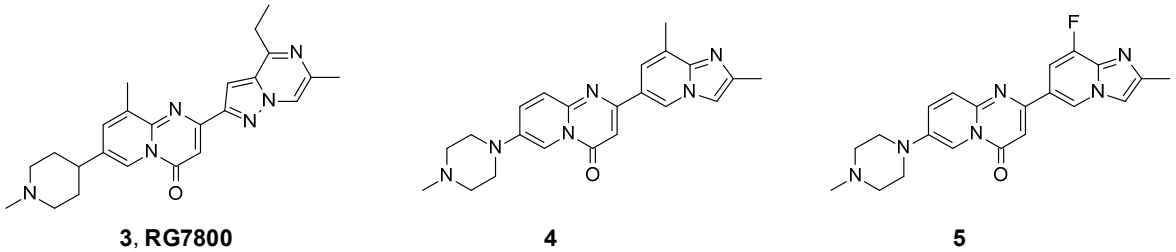

Figure 2. Structures of compounds **3**, **4** and **5**.

RESULTS AND DISCUSSION

Chemistry. The pyrido-pyrimidinone derivatives were prepared using two synthetic routes (Schemes 1 and 2).[11] The first route (Scheme 1) was used specifically for the pyrazolo-pyrazine subclass. N-alkylation of the pyrazole **6** with chloroacetone followed by an intramolecular cyclisation in the presence of ammonium acetate gave the pyrazolo-pyrazine **7**. Chlorination with $POCl_3$ afforded **8**. A Suzuki or a Negishi cross-coupling with either dimethyl

or diethyl zinc led to **9a/b**. A Claisen condensation with *t*-butyl acetate followed by a trans-esterification with ethanol provided the β-keto esters **10a/b**. The key step is a condensation of the β-keto ester **10a/b** with 5-fluoropyridin-2-amine to construct the 2-substituted-7-fluoro-pyrido[1,2-a]pyrimidin-4-one intermediates **11a/b**. A nucleophilic aromatic substitution reaction between **11a** and methyl piperazine gave **12** whereas **13** was obtained by reaction between **11b** and (*S*)-octahydropyrrolo[1,2-a]pyrazine. Alternatively, the condensation of **10a/b** with the substituted 2-amino-pyridines **14** and **19** provided **15**, **16** and **20**, respectively. A reductive amination of **16** with formaldehyde concluded the synthesis of **3**, while a reductive amination of **15** with either formaldehyde or acetaldehyde gave **17** and **18**, respectively.

Scheme 1. Synthesis of the pyrazolo-pyrazine derivatives **3**, **12**, **13**, **15**, **16**, **17**, **18**, and **20**[a]

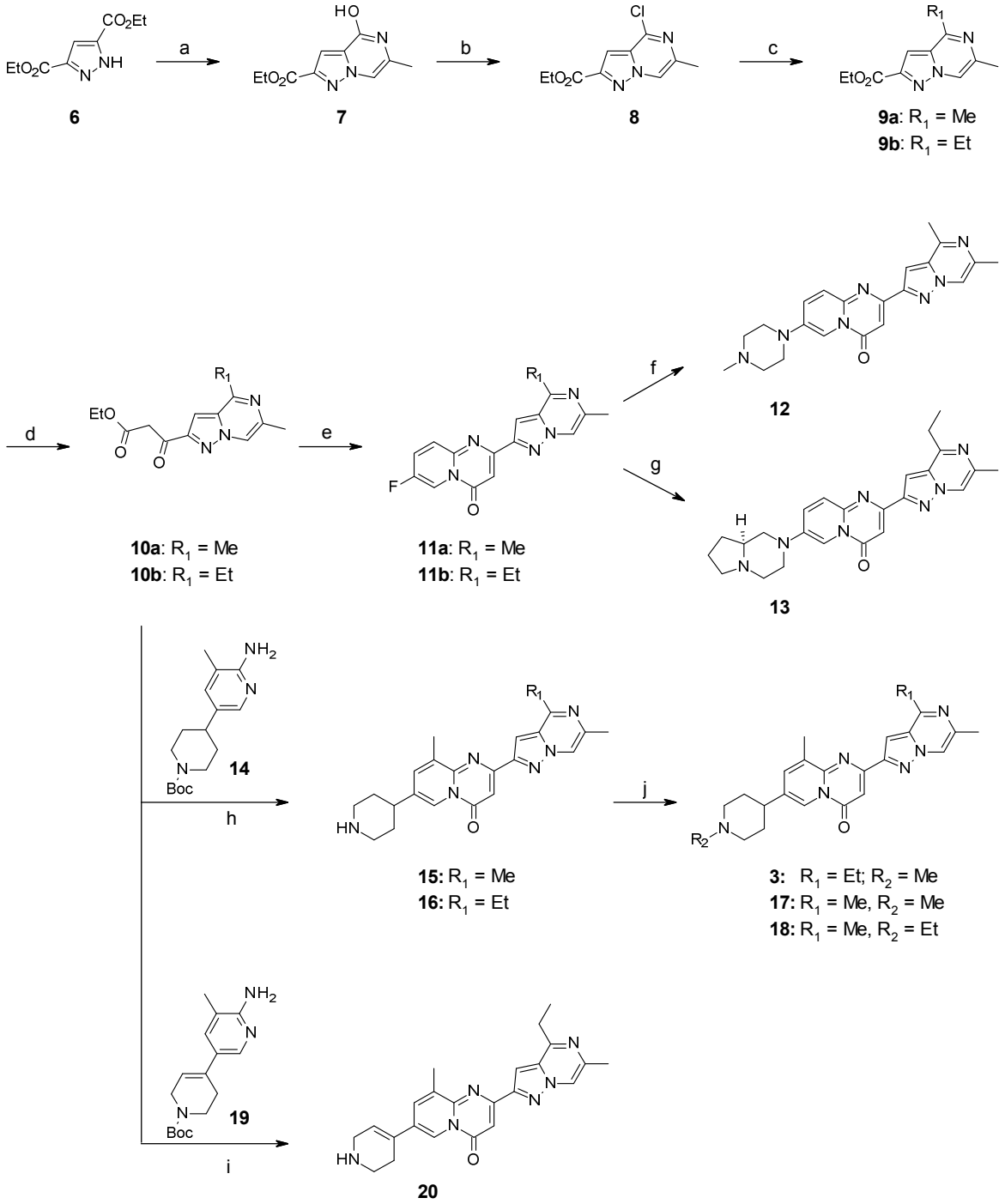

[a] Conditions: a) i. 1-Chloropropan-2-one (1 equiv), K_2CO_3 (1.1 equiv), acetone, 30 °C, 6 h; ii. NH_4OAc (20 equiv), acetic acid, reflux, 48 h, 64% over 2 steps; b) $POCl_3$, reflux, 15 h, 85%; c) Me_2Zn (1.0 equiv), NiCl(dppp) (0.1 equiv), THF, 0 °C, 1 h, 82%; or Et_2Zn (1.0 equiv), NiCl(dppp) (0.05 equiv), THF, 0 °C, 1 h, 80%; d) EtOAc (5 equiv), LiHMDS (2.5 equiv), 77-90%; e) 2-amino-5-fluoro-pyridine (1.2 equiv), PPTS (0.05 equiv), 130 °C, 8 h, 71-86%; f) 1-methylpiperazine (10 equiv), DMA, 120 °C, 15 h, 80%; g) (*S*)-octahydropyrrolo[1,2-a]pyrazine

(2.0 equiv), K_2CO_3 (1.0 equiv), DMSO, 110 °C, 48 h, 63%; h) PPTS (1.1 equiv), 3-methyl-1-butanol, 150 °C, 45 h, 25-39%; i) PPTS (1.0 equiv), 3-methyl-1-butanol, 150 °C, 24 h, 30%; j) HCHO (3.0 equiv), $NaBH(OAc)_3$ (1.5 equiv), CH_2Cl_2, 10 °C, 0.5 h, 47-70%; or acetaldehyde (3.0 equiv), $NaBH(OAc)_3$ (1.5 equiv), CH_2Cl_2, 10 °C, 0.5 h, 90%.

An alternative synthetic route was used to prepare 2-substituted pyrido-pyrimidinones containing a fused 6,5-biaryl system (e.g. imidazo-pyridine, benzoxazole, benzotriazole or benzimidazole) (Scheme 2). A condensation between 5-fluoropyridin-2-amine **21** and dimethyl malonate, followed by chlorination with $POCl_3$ afforded **22**. The right hand side moiety was then introduced by means of a Suzuki cross-coupling between **22** and a wide range of aromatic boronic acids or esters to give **23a-h**. The boronic acid/ester derivatives were commercially available or readily prepared from the corresponding aromatic halide. Finally, an aromatic nucleophilic substitution with a range of secondary amines led to the final derivatives **4**, **5**, and **24-31**.

Scheme 2. Synthesis of derivatives **4**, **5**, and **24-31**[a]

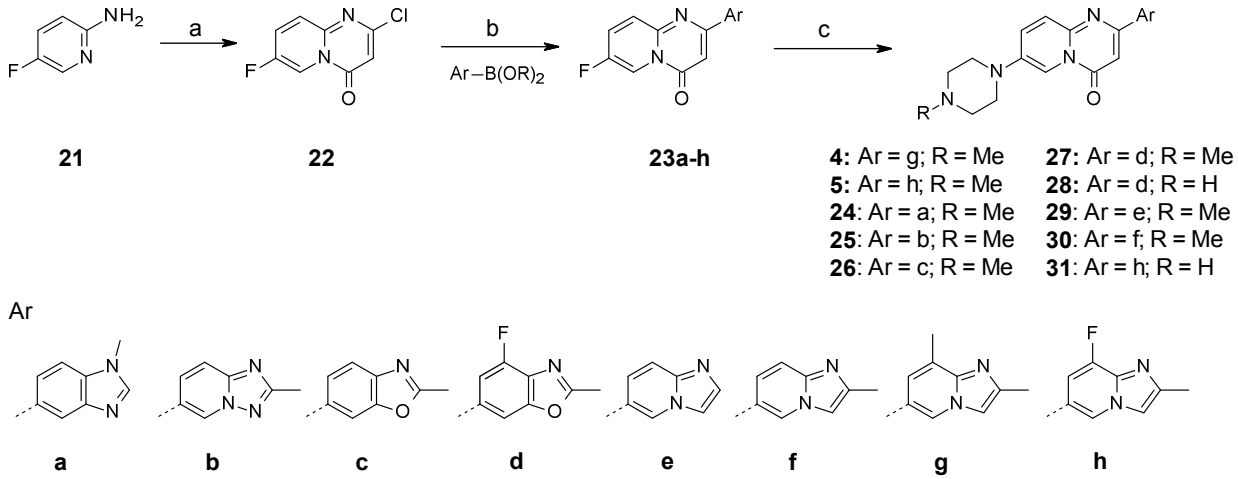

[a] Conditions: a) i. Dimethyl malonate (5 equiv), 230 °C, 1.5 h; ii. $POCl_3$, *i*-Pr_2NEt (1.0 equiv), 110 °C, 15 h, 50% over 2 steps; b) $Pd(dppf)Cl_2$ or $Pd(PPh_3)_4$ (0.05 equiv), aqueous K_2CO_3 (2M, 3.0 equiv), CH_3CN, 50 °C-reflux, 31-97%; c) piperazine or methyl-piperazine (5 equiv), DMA or DMSO, 50-140 °C, 31-66%.

Lead optimization. As spinal muscular atrophy is driven by reduced levels of SMN protein, we aimed to identify a small molecule capable of increasing the level of SMN protein in multiple tissues, including peripheral and central nervous system, upon oral administration. Therefore, in addition to a suitable PK profile, the compounds should not be P-gp substrates. From a safety perspective, although SMA is a terminal disease for its severe form (type 1) without approved therapy, it was important to select a development candidate with no potential for genotoxicity as indicated by the standard Ames assay. The Ames test was considered positive, indicating mutagenicity, when a dose dependent increase in the number of colonies reached at least a 2-fold (strains TA1535, TA98) or 1.5-fold (strains TA97, TA100, TA102) over the background level.

To prevent the genotoxocity observed with the coumarin **1** and its corresponding N-dealkylated metabolite **32**, we either modulated the electronic density of the central core by preparing the aza-coumarin analog **33** or we replaced the right hand side fragment as exemplified by the selected examples **34** and **35** (Figure 3). The aza-coumarin **33** had similar in vitro potency as **1**, however it was also found positive in the Ames assay. The replacement of the imidazo-pyrazine moiety (right hand side fragment) led to derivatives that were negative in the Ames assay. However, both **34** and **35** had poor in vitro potency. Further efforts to identify an Ames-negative compound with high in vitro potency remained unsuccessful in that series.

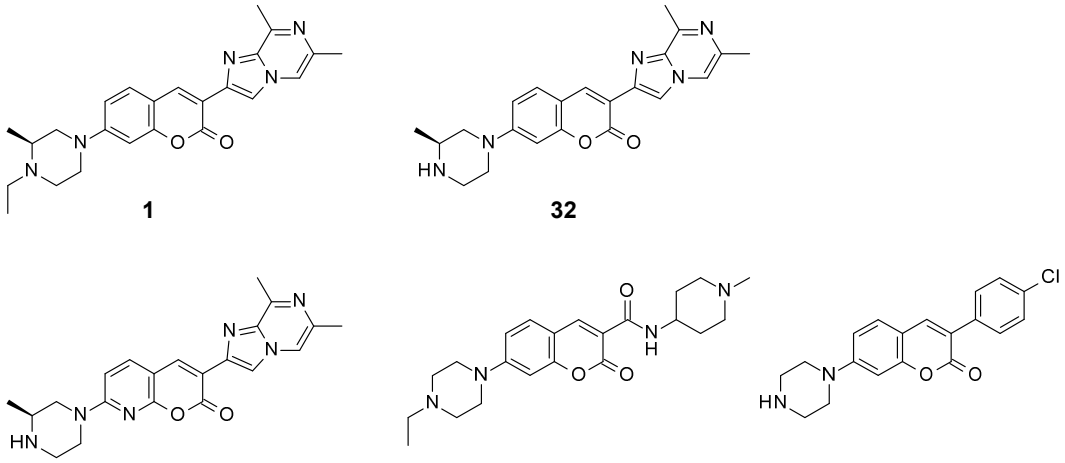

Figure 3. Ames SAR in the coumarin series.

The iso-coumarin **2** and its N-dealkylated metabolite were also found to be positive in the Ames assay. Although not confirmed, we hypothesized that this was most likely due to the presence of the identical imidazo-pyrazine moiety found in coumarin compounds **1**, **32**, and **33**. Compound **2** additionally exhibited pronounced human plasma instability (Figure 4). After a five hour incubation of **2** in human plasma, approximately 55% percent of the parent molecule remained, in contrast to the analogous coumarin compound **1** (Figure 4). This observation pointed towards a ring-opening of the iso-coumarin as the most likely degradation pathway. This hypothesis was strengthened upon replacement of the piperazine moiety by a more electron withdrawing fluorine atom that increased the instability (derivative **36**, 30% remaining). The exchange of the imidazo-pyrazine moiety for an acetyl further increased the instability (derivative **37**, 16%). Our knowledge of the structure activity relationship of the iso-coumarin series indicated that it would not be possible to add an electron rich group on the iso-coumarin core, and therefore we concluded that it would be difficult to increase the plasma stability while maintaining high in vitro potency.

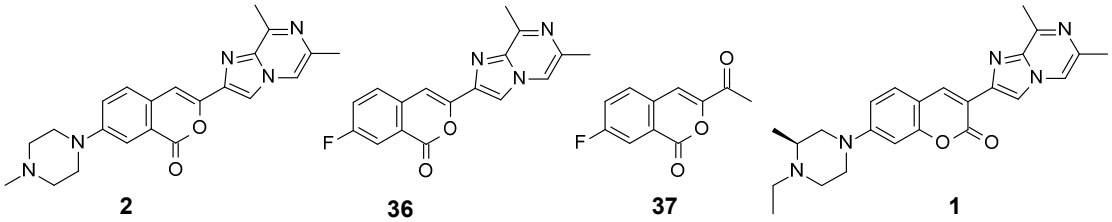

	2	36	37	1
% parent molecule remaining after 5 h incubation in human plasma	55%	30%	16%	93%

Figure 4. Human plasma stability of representative compounds from coumarin and isocoumarin series.

At this stage, it appeared very challenging to further optimize the coumarin and the iso-coumarin series, due to the Ames flag and plasma instability. Additionally, since both coumarin and iso-coumarin moieties are known chromophores that confer phototoxicity,[12] we investigated the selection of an alternative central core (Figure 5). Several bioisosteres were evaluated, such as the isoquinolin-1-one **38** and quinazolin-4-one **39**, and most of them were found to be inactive in vitro. However, the pyrido-pyrimidinone **12** had high in vitro potency (SMN HTRF $EC_{1.5x}$ = 170 nM). Compound **12** was chemically stable in human plasma and aqueous buffer between pH 1 and 12. And while the coumarin **1** and iso-coumarin **2** exhibited strong in vitro phototoxicity with IC_{50} of 80 nM and 150 nM respectively (3T3 assay in the presence of UVA irradiation), the pyrido-pyrimidinone **12** had markedly reduced phototoxicity potential with an IC_{50} of 2,900 nM. The pyrido-pyrimidinone moiety was therefore selected as the central core of choice.

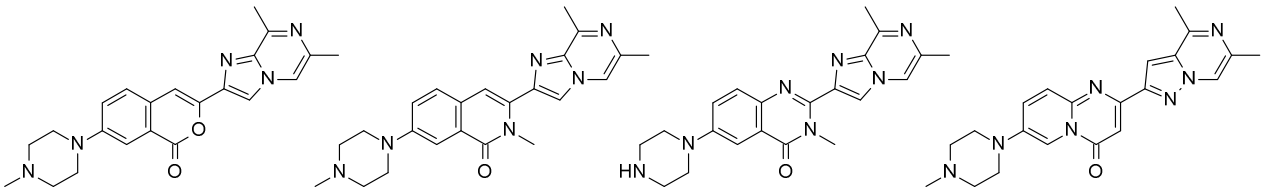

2 **38** **39** **12**

Figure 5. Evaluation of alternative central cores.

Several right hand side fragments in place of the imidazo-pyrazine were evaluated for their in vitro potency and potential mutagenicity (Table 1). As previously observed with the coumarin series, the outcome of the Ames assay was dependent on the right hand side fragment. With the pyrido-pyrimidinone central core, we were able to identify compounds negative in the Ames assay that also demonstrated good in vitro potency by incorporating a pyrazolo-pyrazine moiety as in **12** or a substituted imidazo-pyridine (e.g. **4**, **5** and **31**) as right hand side fragments.

Table 1. Ames assay results and in vitro potency of compounds with a pyrido-pyrimidinone central core and various right hand side fragments R^2.

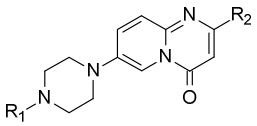

Compd	R^1	R^2	Activity in Ames assay	SMN2 splicing $EC_{1.5x}$ [nM]	SMN protein $EC_{1.5x}$ [nM]
12	Me	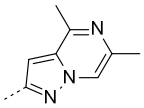	Negative	92	170
24	Me	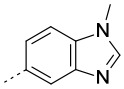	Positive	Inactive	Inactive
25	Me	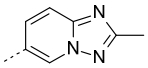	Positive	314	820
26	Me	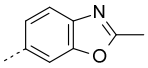	Positive	148	395
27	Me	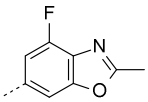	Positive	3	13

28	H		Positive	1	4
29	Me	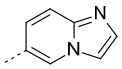	Positive	582	3400
30	Me	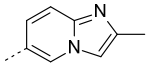	Positive	182	760
4	Me	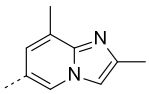	Negative	7	14
5	Me	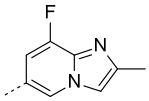	Negative	32	40
31	H	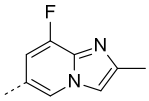	Negative	1	9

Additional analogs around the pyrazolo-pyrazine subseries (analogs of **12**) were prepared and assessed for their in vitro activity and evaluated in the Ames assay (Table 2). Each compound from this subseries was negative in the Ames assay.

Table 2. Ames assay results and in vitro potency within the pyrazolo-pyrazine subseries.

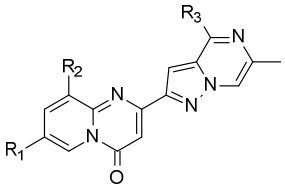

Compd	R^1	R^2	R^3	Activity in Ames assay	*SMN2* splicing $EC_{1.5x}$ [nM]	SMN protein $EC_{1.5x}$ [nM]
12	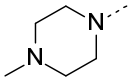	H	Me	Negative	92	170
13	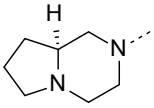	H	Et	Negative	40	163

17	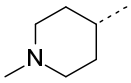	Me	Me	Negative	57	77
3	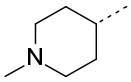	Me	Et	Negative	23	87
18	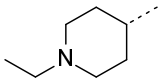	Me	Me	Negative	30	84
20	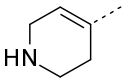	Me	Et	Negative	6	15

An additional objective was to design efficacious compounds leading to increased SMN protein levels in multiple tissues, including peripheral and central nervous system in vivo. Therefore, an important consideration was to prepare derivatives that were not P-glycoprotein (P-gp) substrates. We observed the lipophilicity to be a strong predictor of the efflux ratio (ER, a measure of P-gp efflux; assessed using both human and mouse cells). Compounds were not or only weak P-gp substrates when the measured LogD was greater than 1.6 (Table 2). Compound **18** was described in an earlier manuscript as compound SMN-C3.[7]

Table 2. P-gp efflux ratio and lipophilicity.

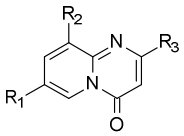

Compd	R^1	R^2	R^3	LogD	Hum P-gp ER	Mouse P-gp ER	SMN protein $EC_{1.5x}$ [nM]
40	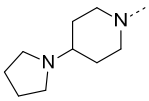	H	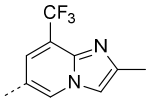	1.45	8.5	14.5	76

41	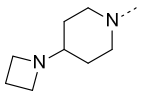	H	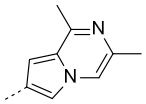	1.53	6.6	10.6	46
17	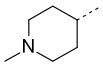	Me	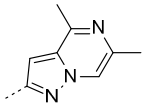	1.82	1.2	2.6	77
18	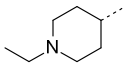	Me	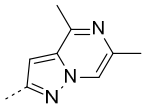	1.87	1.4	2.6	84
3	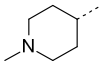	Me	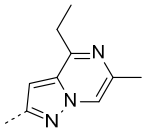	2.26	2.0	2.5	87
5	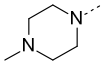	H	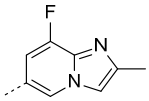	2.30	1.9	2.6	40
27	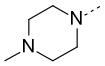	H	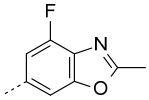	2.46	1.1	1.3	13
4	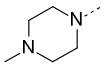	H	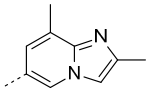	2.49	2.4	3.2	55

In vivo pharmacokinetics and efficacy. At this stage, several compounds that were not P-gp substrates, had good in vitro potency (SMN HTRF $EC_{1.5x}$ < 100 nM), and were negative in the Ames assay were identified. Additional characterization for chemical and human plasma stability, aqueous solubility (Thesa, FaSSIF and FeSSIF), permeability (Pampa), DDI (drug-drug interaction CYP3A4, 1A2, 2C9, 2C19 and 2D6), TDI (time dependent inhibition, CYP3A4), in vitro clearance (liver microsomes and hepatocytes) and absence of covalent binding (CVB) prompted us to evaluate compounds **3, 4** and **5** further. The three compounds demonstrated a favorable drug metabolism and pharmacokinetics (DMPK) profile in the rat and in cynomolgus monkey with good oral bioavailability. A much longer half-life for compound **3** relative to **4** and **5** was observed, consistent with a higher volume of distribution (Table 3). Compounds **4** and **5** have a similar fraction unbound in plasma across species (fu_p for **4**: human, cyno, rat, mouse:

11%, 8%, 10% and 16%, respectively, and fu_p for **5**: human, cyno, rat, mouse: 22%, 18%, 16% and 17%, respectively) whereas for **3** a markedly lower free fraction in mouse was measured (fu_p human, cyno, rat, mouse: 13%, 16%, 17% and 2%, respectively).

Table 3. In vivo SDPK profile for compounds **3** - **5**

Compd	rat				Cyno			
	Cl[a] (mL/min/kg)	Vss[a] (l/kg)	$T_{1/2}$[b] (h)	F[b] (%)	Cl[c] (mL/min/kg)	Vss[c] (l/kg)	$T_{1/2}$[d] (h)	F[d] (%)
3	18	20	12	83	5	20	40-60	52
4	38	14	~ 6	55-100	7.5	4.3	~ 8	~ 100
5	61	5	4	~ 100	9.7	2.4	2.9	84

a) iv: 2 mg/kg; b) PO: 10 mg/kg; c) iv: 0.3 mg/kg; d) PO: 1 mg/kg.

We next evaluated the small molecule splicing modifiers **3**, **4** and **5** in disease models of SMA. For this purpose we used the adult C/C-allele SMA mouse model, in which the animals have a mild SMA phenotype, a normal life span, but show muscle weakness, reduced body weight gain and peripheral necrosis. Compounds **3**-**5** were administered orally once daily (qd) for 10 days at three different doses (1, 3 and 10 mg/kg). One hour after the final dose tissues were collected from the mice and the level of the SMN protein was determined in brain and quadriceps muscle. All three compounds showed a clear dose dependent increase in SMN protein levels (Table 4).

Table 4. Pharmacokinetics and SMN induction in adult C/C-allele mouse model

Compd	Dose (mg/kg PO)	Total Plasma[a] AUC (μg·h/mL)	Free Plasma AUC (μg·h/mL)	% SMN indu. in brain	% SMN indu. in quadriceps
Vehicle	0	0	0	0	0
3	1			7	30

3	3			19	57
3	10	33	0.66	122	94
4	1			0	28
4	3			0	70
4	10	2.5	0.40	39	133
5	1			42	40
5	3			60	81
5	10	2.7	0.45	141	126

[a] Plasma AUC determined in a satellite group

These splicing modifiers were then tested in Δ7 SMA mice, a model of severe SMA, where animals die within three weeks after birth.[13] Dosing was initiated with compounds **3-5** by intraperitoneal (i.p.) injection once daily starting on postnatal day 3 (P3) and continued through day 9 (P9). One hour after the last dose, the level of the SMN protein was determined in brain and quadriceps muscle (Table 5). All three compounds dose-dependently increased SMN protein level in the brain and in peripheral tissue (quadriceps muscle).

Table 5. Pharmacokinetics and SMN induction in neonatal Δ7 mouse model

Compd	Dose (mg/kg ip)	Total Plasma[a] AUC (μg·h/mL)	Free Plasma AUC (μg·h/mL)	% SMN indu. in brain	% SMN indu. in quadriceps
Vehicle	0	0	0	0	0
3	0.3			20	40
3	1			55	57
3	3	5.9	0.118	135	160
4	0.3			39	31
4	1			130	115
4	3	1.3	0.208	162	130
5	0.1			72	107

5	0.3			116	189
5	1	4.3	0.721	159	260

[a] Plasma AUC determined in a satellite group of neonatal (P10) wild-type mice. (The free-fraction measured using serum from adult mice was used to calculate the free plasma AUC.

Finally, we assessed the impact of treatment with SMN2 splicing modifiers on the lifespan and body weight of Δ7 SMA mice. Mice were treated with compounds **3** and **4** at 0.3, 1 and 3 mg/kg/day by i.p. injections from P3 through P23, and thereafter at 1, 3 and 10 mg/kg/day, respectively, by oral gavage. Compound **5** was administered at 0.03, 0.1, 0.3 and 1 mg/kg/day by i.p injections from P3 through P23, and thereafter at 0.1, 0.3, 1 and 3 mg/kg/day, respectively, by oral gavage (Figure 7). Survival and body weight were assessed daily. While all vehicle-treated mice died less than three weeks after birth, mice treated with **3** and **4** demonstrated a dose-dependent increase in survival beginning at the low dose (0.3/1 mg/kg). In the mid and high dose groups (1/3 and 3/10 mg/kg, respectively), approximately 80 to 90% of animals survived beyond P50/P60 with profound body weight gain when the study was terminated. Compound **5** showed a similar effect on survival and body weight gain, initiating at an even lower dose.

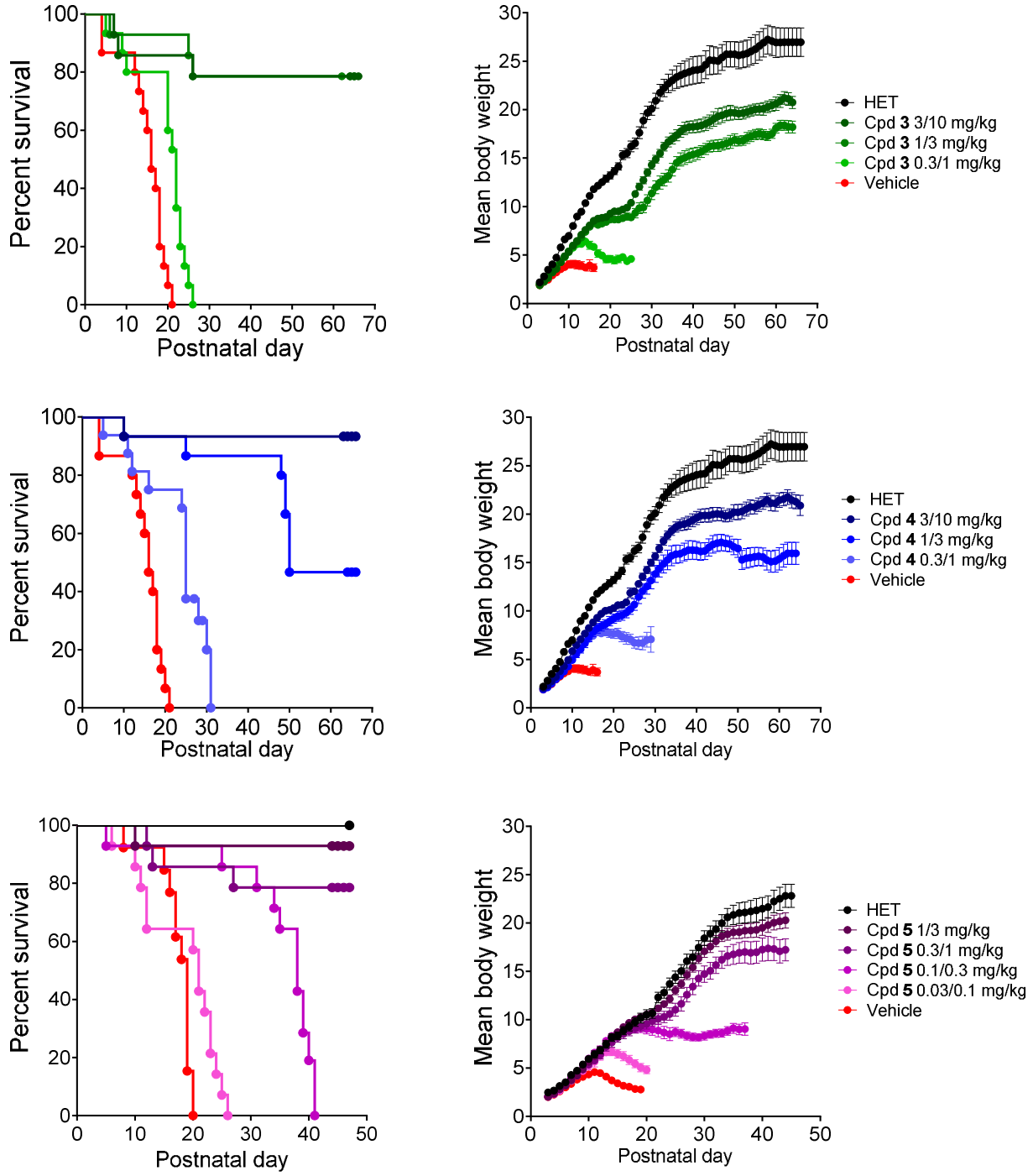

Figure 7. Survival and body weight gain of Δ7 mice treated with compounds **3**, **4** and-**5**. Animals were treated with vehicle or compound at doses of 0.3, 1, or 3 mg/kg/day from PND3-PND23 by IP injection, and thereafter by oral gavage at doses of 1, 3, or 10 mg/kg/day from

PND24 through PND65. Data represent means ± SEM of an initial group size of 10 (HET), 15 (SMNΔ7 SMA mice, vehicle or compound -treated).

Further characterization of compound **3** was then performed to demonstrate that those small molecules are increasing the SMN protein level via inducing alternative splicing of the SMN2 mRNA both in vitro and in vivo. Compound **3** was shown to promote the inclusion of exon 7 in SMN2 mRNA generating full length (FL) mRNA in vitro using fibroblasts from an SMA type 1 patient (Figure 8, panel A). To investigate SMN protein production as a consequence of splicing correction, an in vitro assay assessed the levels of SMN protein in fibroblasts and in spinal motor neurons derived from SMA Type I and II patient induced pluripotent stem cells (iPSC). The maximal increase in SMN protein produced, compared to untreated controls, was similar in both cell types (60-80%; Figure 8, panels B and C), suggesting that in different cell types derived from SMA patients, compound **3** increases SMN protein level as a result of correcting the dysfunctional SMN2 splicing in vitro.

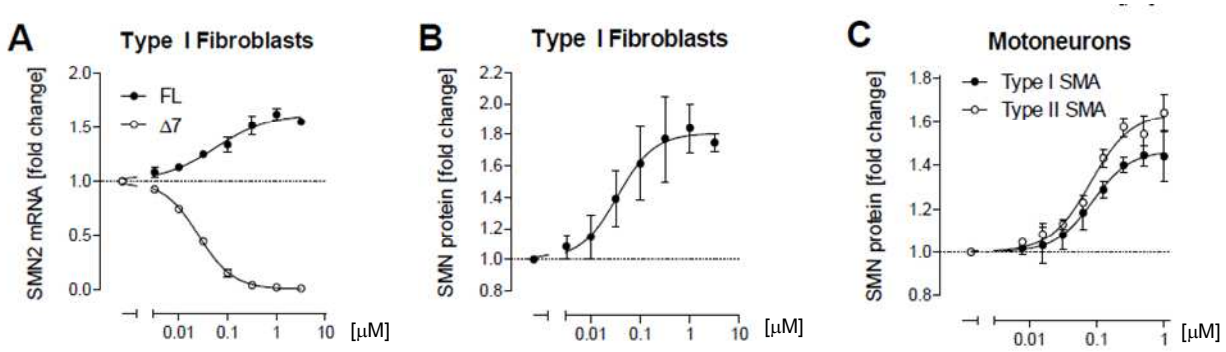

Figure 8: Compound **3** tested in: **A**. SMN2 splicing in SMA type 1 fibroblasts. **B**. SMN protein in SMA type 1 fibroblasts. **C**. SMN protein in SMA type I and II motor neurons. FL, full length, Δ7, mRNA lacking exon 7.

For assessment of the in vivo effects of compound **3** on SMN2 splicing, adult SMA model mice (C/C-allele) were treated for 10 days with vehicle or compound **3** (3 or 10 mg/kg po once daily). Compound **3** dose dependently corrected SMN2 splicing by including exon 7 to create FL mRNA (Figure 9, panel A), suggesting that compound **3** corrects alternative splicing of the human SMN2 gene in the brain of transgenic SMA mice model, leading to an increase of the SMN protein in brain (Figure 9, panel B).

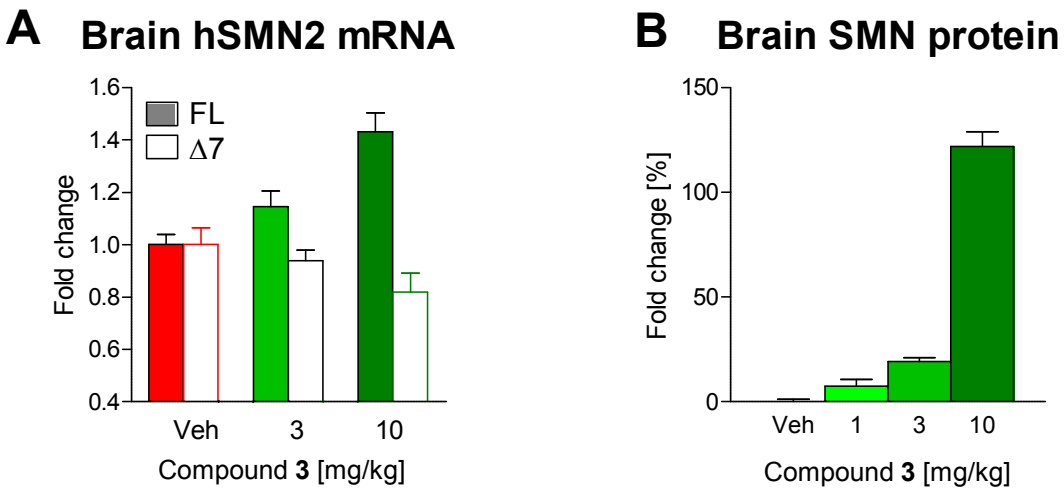

Figure 9: Compound **3** induces SMN2 splicing (panel A) and SMN protein increase (panel B) in C/C-allele mice.

CONCLUSION

In summary, chemical optimization of the pyrido-pyimidinone class for safety parameters (Ames), DMPK profile (P-gp, plasma and chemical stability) and pharmacology (in vitro / in vivo potency) has led to the discovery of orally available small molecule compounds that specifically modify the alternative splicing of *SMN2* exon 7 in SMA patient-derived cells and in two SMA mouse models. This splicing modification results in a clear functional benefit in mice

that model a severe SMA form. Compounds **3-5** exhibited excellent pharmacokinetic and in vivo efficacy and had a favorable safety profile.

These results suggested that our splicing modifier compounds could provide a therapeutic benefit for SMA patients. On this basis, compound **3** from the pyrazolo-pyrazine subclass entered clinical development. This represents the first clinical trial with a small molecule splicing modifier in SMA, enlarging the path for the treatment of other diseases via modulation of pre-mRNA splicing. An eye finding in a non-human primates safety study led us to put on hold our clinical trial with that molecule. The complete safety characterization of **3** and the outcome of the clinical trials will be reported in future publications.

EXPERIMENTAL SECTION

Compound Synthesis and Characterization. Chemistry.

Reactions were carried out under argon atmosphere. Unless otherwise mentioned, all reagents and chemicals were obtained from commercial suppliers and used without further purification. All reactions were followed by TLC (TLC plates F254, Merck) or LCMS (liquid chromatography-mass spectrometry) analysis. The purity of final compounds as measured by HPLC was at least above 95%. Flash column chromatography was carried out either using cartridges packed with silica gel (Isolute Columns, Telos Flash Columns) or on glass columns on silica gel 60 (32-60 mesh, 60Å). LC high resolution spectra were recorded with a Agilent LC-system consisting of Agilent 1290 high pressure system, a CTC PAL auto sampler and a Agilent 6520 QTOF. The separation was achieved on a Zorbax Eclipse Plus C18 1,7 µm 2.1*50mm column at 55°C; A=0.01% formic acid in Water; B= 0.01% formic acid in acetonitrile at flow 1

mL/min. gradient: 0 min 5%B, 0.3 min 5%B, 4.5 min 99 %B 5 min 99%B. The NMR spectra were measured on a Bruker 600 MHz machine in a 5 mm TCI cryoprobe at 298 K. TMS was used for referencing for experiment done in $CDCl_3$. The deuterated DMSO-d6 solvent signal was used as reference with 2.50 ppm.

2-(4-Ethyl-6-methyl-pyrazolo[1,5-a]pyrazin-2-yl)-9-methyl-7-(1-methyl-4-piperidyl) pyrido[1,2-a]pyrimidin-4-one (**3**). According to scheme 1: *Step A*. Preparation of **7**. (i) To a solution of diethyl 1H-pyrazole-3,5-dicarboxylate **6** (10.0 g, 47 mmol) and 1-chloropropan-2-one (3.76 mL, 47 mmol) in acetone (200 mL) was added K_2CO_3 (7.2 g, 52 mmol). The reaction mixture was heated at 30 °C for 6 hours, and concentrated in vacuo to remove the volatiles. The residue was dissolved in EtOAc and washed with water. The organic phase was dried over $MgSO_4$ and concentrated to give diethyl 1-(2-oxopropyl)-1H-pyrazole-3,5-dicarboxylate as a light brown solid, which was used directly in the next step. (ii) The crude product was dissolved in acetic acid (300 mL) and NH_4OAc (72 g, 0.940 mol) was added. After refluxing for 48 h, the mixture was concentrated and diluted with water. The precipitate was collected by filtration, washed with cold water and CH_3CN to give ethyl 4-hydroxy-6-methyl-pyrazolo[l,5- a]pyrazine-2-carboxylate **7** (6.7 g, 64%) as an off-white solid. ^{1}H NMR (600 MHz, DMSO-*d*6) δ ppm: 11.51 (br s, 1H), 7.62 (d, *J*=0.9 Hz, 1H), 7.32 (d, *J*=0.7 Hz, 1H), 4.32 (q, *J*=7.2 Hz, 2H), 2.14 (d, *J*=1.1 Hz, 3H), 1.31 (t, *J*=7.1 Hz, 3H); LC-HRMS: m/z=221.08093 [(M+H)+ calcd for $C_{10}H_{11}N_3O_3$: 221.08004; Diff 0.9 mDa].

Step B. Preparation of **8**. Ethyl 4-hydroxy-6-methylpyrazolo [1,5 -a]pyrazine-2-carboxylate **7** (7.18 g, 32.5 mmol) was dissolved in $POC1_3$ (80 mL) and heated at reflux for 15 hours. The dark mixture was cooled to RT, concentrated in vacuo to form a precipitate which

was collected by filtration and washed with CH_3CN to give ethyl 4-chloro-6-methylpyrazolo[1,5-a]pyrazine-2- carboxylate **8** (5.197 g) as an off-white solid. The filtrate was concentrated and purified by column chromatography to give an additional fraction (1.42 g) of **8** and a combined yield of 85%. ^{1}H NMR (600 MHz, DMSO-*d*6) δ ppm: 8.80 (t, *J*=1.0 Hz, 1H), 7.41 (d, *J*=1.0 Hz, 1H), 4.38 (q, *J*=7.2 Hz, 2H), 2.45 (d, *J*=0.9 Hz, 3H), 1.34 (t, *J*=7.1 Hz, 3H); LC-HRMS: m/z=239.0461 [(M+H)+ calcd for $C_{10}H_{10}ClN_3O_2$: 239.04615; Diff -0.1 mDa].

Step C. Preparation of **9-b**. To a solution of 4-chloro-6-methylpyrazolo[1,5-a]pyrazine-2-carboxylate **8** (10 g, 41 mmol) in THF (150 mL) was added [1,3-bis(diphenylphosphino)propane]nickel(II) chloride (1.13 g, 2.08 mmol). The yellowish suspension was cooled to 0 °C and diethyl zinc (43.2 mL, 1.1 M in toluene, 47.5 mmol) was added over 40 minutes and stirring continued for an additional 30 minutes. Water (5 mL) diluted in THF (20 mL) was added dropwise at 0 °C (very exothermic reaction) and the reaction mixture concentrated in vacuo. The residue was dissolved in EtOAc (150 mL) and washed with brine (150 mL). The organic phase was dried over $MgSO_4$ and the product was purified by column chromatography (SiO_2, EtOAc/Heptane 1:1) to give ethyl 4-ethyl-6-methyl-pyrazolo[1,5-a]pyrazine-2-carboxylate **9-b** (7.65 g, 80%) as a light yellow solid. ^{1}H NMR (600 MHz, DMSO-d_6) δ ppm: 8.54 (s, 1H), 7.50 (d, *J*=1.0 Hz, 1H), 4.36 (q, *J*=7.2 Hz, 2H), 3.06 (q, *J*=7.5 Hz, 2H), 2.44 (d, *J*=0.9 Hz, 3H), 1.34 (t, *J*=7.1 Hz, 3H), 1.30 (t, *J*=7.5 Hz, 3H); LC-HRMS: m/z=233.1178 [(M+H)+ calcd for $C_{12}H_{15}N_3O_2$: 233.11643; Diff 1.4 mDa].

Step D. Preparation of **10-b**. To a solution of ethyl 4-ethyl-6-methyl-pyrazolo[1,5-a]pyrazine-2-carboxylate **9-b** (6.6 g, 28.3 mmol) in THF (370 mL) was added EtOAc (13.5 mL, 141 mmol). The reaction mixture was cooled down to -30 °C before LiHMDS (70.7 mL, 1M in THF, 70.7 mmol) was added slowly over 20 minutes. Stirring was continued for an additional 30

minutes at -30 °C, and the reaction mixture was quenched by addition of an aqueous saturated NH_4Cl solution (50 mL). The reaction mixture was poured in EtOAc (300 mL) and washed with water. The organic phase was dried over Na_2SO_4 and concentrated in vacuo. The crude material was purified by chromatography (SiO_2, CH_2Cl_2/EtOAc: 9:1 to 4:1) to give ethyl 3-(4-ethyl-6-methyl-pyrazolo[1,5-a]pyrazin-2-yl)-3-oxo-propanoate **10-b** (7.01 g, 90%) as a light yellow solid.

Step H. Preparation of **16**. A stirred solution of ethyl 3-(4-ethyl-6-methylpyrazolo[1,5-a]pyrazin-2-yl)-3-oxo-propanoate **10-b** (8.14 g, 29.6 mmol), tert-butyl 4-(6-amino-5-methylpyridin-3-yl)piperidine-1-carboxylate (8.62 g, 29.6 mmol) and pyridinium p-toluene sulfonate (8.17 g, 32.5 mmol) in 3-methyl-1-butanol (82 mL) was heated at 150 °C for 45 hours. The volatiles were removed in vacuo and the residue poured into 350 mL CH_2Cl_2 and washed with an aqueous solution of NaOH (0.5 M, 200 mL). The organic phase was dried over Na_2SO_4 and concentrated in vacuo. The crude product was purified by column chromatography (SiO_2, CH_2Cl_2/MeOH 95:5 to 9:1) to give 2-(4-ethyl-6-methyl-pyrazolo[1,5-a]pyrazin-2-yl)-9-methyl-7-(4-piperidyl)pyrido[1,2-a] pyrimidin-4-one **16** (3.05 g, 25%) as an off-white solid. ^{1}H NMR (600 MHz, DMSO-*d*6) δ ppm: 8.68 (s, 1H), 8.56 (s, 1H), 7.92 (s, 1H), 7.60 (d, *J*=0.9 Hz, 1H), 6.99 (s, 1H), 3.07 - 3.14 (m, 3H), 3.07 - 3.14 (m, 1H), 2.74 - 2.84 (m, 1H), 2.63 - 2.67 (m, 3H), 2.62 - 2.70 (m, 2H), 2.45 (s, 3H), 1.83 (br d, *J*=13.0 Hz, 2H), 1.58 (qd, *J*=12.3, 3.8 Hz, 2H), 1.34 (t, *J*=7.6 Hz, 3H); LC-HRMS: m/z=402.21862 [(M+H)+ calcd for $C_{23}H_{26}N_6O$: 402.21681; Diff 1.8 mDa].

Step J. To a suspension of 2-(4-ethyl-6-methyl-pyrazolo[1,5-a]pyrazin-2-yl)-9-methyl-7-(4-piperidyl)pyrido[1,2-a]pyrimidin-4-one **16** (5.79 g, 14.4 mmol) in CH_2Cl_2 (91 mL) cooled down to 5-10 °C, was added sodium triacetoxyborohydride (4.7 g, 21.6 mmol) and a

formaldehyde solution (3.22 mL, 37 wt% in H_2O, 43.2 mmol) dropwise over 5-10 minutes. After an additional 30 minutes, the reaction was quenched by addition of an aqueous saturated solution of K_2CO_3 (30 mL). The reaction mixture was poured into 500 mL of CH_2Cl_2 and washed with brine. The organic phase was dried over Na_2SO_4 and concentrated in vacuo. The crude material was purified by column chromatography (SiO_2, CH_2Cl_2/MeOH 9:1 to 4:1) to give 2-(4-ethyl-6-methyl-pyrazolo[1,5-a]pyrazin-2-yl)-9-methyl-7-(1-methyl-4-piperidyl)pyrido[1,2-a]pyrimidin-4-one **3** (4.05 g ,69%) as an off-white solid. ^{1}H NMR (600 MHz, CHLOROFORM-d) δ ppm: 8.86 (d, *J*=1.7 Hz, 1H), 8.12 (s, 1H), 7.59 (s, 1H), 7.44 (d, *J*=1.0 Hz, 1H), 7.27 (s, 1H), 3.00-3.15 (m, 4H), 2.72 (s, 3H), 2.57 - 2.67 (m, 1H), 2.54 (d, *J*=0.9 Hz, 3H), 2.39 (br s, 3H), 2.16 (br s, 2H) 1.93 (br s, 4H), 1.45 (t, *J*=7.6 Hz, 3H); LC-HRMS: m/z=416.23403 [(M+H)+ calcd for $C_{24}H_{28}N_6O$: 416.23357; Diff 1.1 mDa].

2-(2,8-Dimethylimidazo[1,2-a]pyridin-6-yl)-7-(4-methylpiperazin-1-yl)pyrido[1,2-a]pyrimidin-4-one (**4**). According to scheme 2: *Step A*. Preparation of **22**. (i) A mixture of 2-amino-5-fluoropyridine **21** (11.20 g, 0.10 mol) and dimethyl malonate (57.0 mL, 0.50 mol) was heated at 230 °C for 1.5 hours. After cooling to RT, the precipitate was collected by filtration and washed with CH_3CN to give 7-fluoro-2- hydroxy-4H-pyrido[1,2-a]pyrimidin-4-one as a light brown solid, which was used directly in the next step. (ii) A mixture of crude 7-fluoro-2-hydroxy-4H-pyrido[1,2- a]pyrimidin-4-one in $POC1_3$ (50 mL) and *i*-Pr_2NEt (13.3 mL, 77 mmol) was heated at 110 °C for 15 hours. The volatiles were removed and the dark residue was treated with ice-water, washed with water (3x) and dried to give a brown solid. The crude brown solid was purified by column chromatography (SiO_2, CH_2C1_2/MeOH 95:5) to give 2-chloro-7-fluoro-pyrido[1,2-a]pyrimidin-4-one **22** (9.84 g, 50%) as a yellow solid. ^{1}H NMR (600 MHz, DMSO-

*d*6) δ ppm: 8.99 (dd, *J*=4.7, 2.9 Hz, 1H), 8.25 (ddd, *J*=9.8, 7.1, 2.9 Hz, 1H), 7.85 (dd, *J*=9.7, 5.3 Hz, 1H), 6.56 (s, 1H); LC-HRMS: m/z=198.00032 [(M+H)+ calcd for $C_8H_4ClFN_2O$: 197.99962; Diff 0.7 mDa].

Step B. Preparation of **23-g**. To a solution of 2,8-dimethyl-6-(4,4,5,5-tetramethyl-1,3,2-dioxaborolan-2-yl)imidazo[1,2-a]pyridine (6.91 g, 25.4 mmol) in CH_3CN (240 mL) was added $Pd(Ph_3P)_4$ (1.22 g, 1.06 mmol), 2-chloro-7-fluoro-pyrido[1,2-a]pyrimidin-4-one **22** (4.2 g, 21.1 mmol) and an aqueous solution of K_2CO_3 (21.1 mL, 2M, 21.1 mmol). The reaction mixture was heated at 80 °C for 7 hours and concentrated in vacuo. Purification of the residue by column chromatography (SiO_2, CH_2Cl_2/MeOH 98:2 to 95:5) gave 2-(2,8-dimethylimidazo[1,2-a]pyridin-6-yl)-7-fluoro-pyrido[1,2-a]pyrimidin-4-one **23-g** (4.57 g, 70%) as a light yellow solid.

Preparation of 2,8-dimethyl-6-(4,4,5,5-tetramethyl-1,3,2-dioxaborolan-2-yl)imidazo[1,2-a] pyridine: (i) A solution of 5-bromo-3-methylpyridin-2-amine (10 g, 51.9 mmol) and chloroacetone (5.22mL, 62.2 mmol) in CH_3CN (100 mL) was heated at 110°C for 6 hours and then at 100 °C overnight. The reaction was cooled down to RT before an aqueous saturated solution of $NaHCO_3$ (200 mL) was added. The product was extracted several times with EtOAc, the combined organic phases were dried over $MgSO_4$ and purification by column chromatography (SiO_2, EtOAc/Heptane 1:2) gave 6-bromo-2,8-dimethyl-imidazo[1,2-a]pyridine (9.46 g, 81%) as a light brown solid. (ii) A solution of 6-bromo-2,8-dimethylimidazo[1,2-a]pyridine (1.00 g, 4.44 mmol), 4,4,4',4',5,5,5',5'-octamethyl-2,2'-bi(1,3,2-dioxaborolane) (1.24 g, 4.89 mmol), potassium acetate (872 mg, 8.89 mmol) and $PdCl_2$(DPPF)-CH_2Cl_2 (163 mg, 0.222 mmol) in dioxane (35 mL) was heated at 80 °C overnight. The reaction mixture was cooled down to RT, filtered through a pad of celite, concentrated under vacuo and the residue was used directly in the next step without further purification.

Step C. To a solution of 2-(2,8-dimethylimidazo[1,2-a]pyridin-6-yl)-7-fluoro-pyrido[1,2-a]pyrimidin-4-one **23-g** (6.4 g, 20.8 mmol) in DMSO (120 mL) was added K_2CO_3 (2.87 g, 20.8 mmol) and 1-methylpiperazine (6.91 mL, 62.3 mmol). The reaction mixture was heated at 110 °C for 48 hours. The reaction was concentrated under vacuo and the residue purified by column chromatography (SiO_2, CH_2Cl_2/MeOH 98:2 to to 9:1) to give 2-(2,8-dimethylimidazo[1,2-a]pyridin-6-yl)-7-(4-methylpiperazin-1-yl)pyrido[1,2-a]pyrimidin-4-one **4** (4.76 g, 59%) as a yellow solid. ^{1}H NMR (600 MHz, DMSO-d_6) δ ppm 9.20 (s, 1 H), 8.25 (d, *J*=2.6 Hz, 1 H), 8.10 (dd, *J*=9.7, 2.8 Hz, 1H), 7.78 (d, *J*=4.1 Hz, 1H), 7.77 - 7.79 (m, 1H), 7.70 (d, *J*=9.7 Hz, 1H), 6.94 (s, 1H), 3.22 - 3.29 (m, 4H), 2.53 - 2.66 (m, 4H), 2.52 (s, 3 H), 2.36 (s, 3 H), 2.24 - 2.34 (m, 3 H); LC-HRMS: m/z=388.19897 [(M+H)+ calcd for $C_{22}H_{24}N_6O$: 388.201159448; Diff -2.2 mDa].

2-(8-Fluoro-2-methyl-imidazo[1,2-a]pyridin-6-yl)-7-(4-methylpiperazin-1-yl)pyrido [1,2-a]pyrimidin-4-one (5). According to scheme 2: Step B. Preparation of 23-h. To a solution of 8-fluoro-2-methyl-6-(4,4,5,5-tetramethyl-1,3,2-dioxaborolan-2-yl)imidazo[1,2-a]pyridine (5.18 g, 18.8 mmol) in acetonitrile (160 mL) was added $Pd(Ph_3P)_4$ (1.08 g, 0.94 mmol), 2-chloro-7-fluoro-pyrido[1,2-a]pyrimidin-4-one 22 (4.47 g, 22.5 mmol) and an aqueous solution of K_2CO_3 (18.8 mL, 2M, 37.6 mmol). The reaction mixture was heated at 80 °C for 5 hours and concentrated in vacuo. Purification of the residue by column chromatography (SiO2, CH_2Cl_2/MeOH 98:2 to 95:5) gave 7-fluoro-2-(8-fluoro-2-methyl-imidazo[1,2-a]pyridin-6-yl)pyrido[1,2-a]pyrimidin-4-one 23-h (3.59 g, 51%) as a light yellow solid.

Preparation of 8-fluoro-2-methyl-6-(4,4,5,5-tetramethyl-1,3,2-dioxaborolan-2-yl)imidazo[1,2-a]pyridine: (i) An orange solution of 5-bromo-3-fluoropyridin-2-amine (5.20 g, 27.2 mmol), PPTS (0.684 g, 2.72 mmol) and 1-bromo-2,2-dimethoxypropane (4.05 mL, 29.9 mmol) in 2-

propanol (65 mL) was heated at 80 °C overnight. The reaction was cooled down to RT before an aqueous saturated solution of $NaHCO_3$ (100 mL) was added. The product was extracted several times with EtOAc, the combined organic phases were dried over $MgSO_4$ and purification by column chromatography (SiO_2, EtOAc/Heptane 1:4 to 1:1) gave 6-bromo-8-fluoro-2-methyl-imidazo[1,2-a]pyridine (4.80 g ,77%) as a yellow solid. (ii) A solution of 6-bromo-8-fluoro-2-methyl-imidazo[1,2-a]pyridine (1.58 g, 6.90 mmol), 4,4,4',4',5,5,5',5'-octamethyl-2,2'-bi(1,3,2-dioxaborolane) (2.21 g, 8.69 mmol), potassium acetate (2.03 g, 20.7 mmol) and $PdCl_2$(DPPF)-CH_2Cl_2 (282 mg, 0.345 mmol) in dioxane (32 mL) was heated at 90 °C for 5 hours. The reaction mixture was cooled down to RT, filtered through a pad of celite, concentrated in vacuo and the residue was used directly in the next step without further purification.

Step C. To a solution of 7-fluoro-2-(8-fluoro-2-methyl-imidazo[1,2-a]pyridin-6-yl)pyrido[1,2-a]pyrimidin-4-one **23-h** (145 mg, 0.46 mmol) in DMSO (2.0 mL) was added K_2CO_3 (96 mg, 0.697 mmol) and 1-methylpiperazine (0.15 mL, 1.39 mmol). The reaction mixture was heated at 120 °C for 7 hours. The reaction was concentrated in vacuo and the residue purified by column chromatography (SiO_2, CH_2Cl_2/MeOH 98:2 to to 9:1) to give 2-(8-fluoro-2-methyl-imidazo[1,2-a]pyridin-6-yl)-7-(4-methylpiperazin-1-yl)pyrido[1,2-a]pyrimidin-4-one **5** (75 mg, 42%) as a yellow solid. ^{1}H NMR (600 MHz, CHLOROFORM-d) δ ppm: 8.77 (d, *J*=1.4 Hz, 1H), 8.43 (d, *J*=2.6 Hz, 1H), 7.70 (d, *J*=2.7 Hz, 1H), 7.61 – 7.67 (m, 1H), 7.46 – 7.52 (m, 2H), 6.75 (s, 1H), 3.24 - 3.38 (m, 4H), 2.65 (br s, 4H), 2.51 (d, *J*=0.7 Hz, 3H), 2.40 (d, 3H); LC-HRMS: m/z=392.17532 [(M+H)+ calcd for $C_{21}H_{21}FN_6O$: 392.17609; Diff 0.77 mDa].

2-(4,6-Dimethylpyrazolo[1,5-a]pyrazin-2-yl)-7-(4-methylpiperazin-1-yl)pyrido[1,2-a]pyrimidin-4-one (**12**). According to scheme 1: *Step C*. Preparation of **9-a**. To a suspension of

ethyl 4-chloro-6-methylpyrazolo[1,5-a]pyrazine-2-carboxylate **8** (6.7 g, 28.0 mmol) in THF (265 mL) at 0 °C was added dimethylzinc (28.0 mL, 28.0 mmol) and 1,3-bis(diphenylphosphino)propane-nickel(II) chloride (1.52 g, 2.8 mmol). The temperature was raised to RTand the reaction stirred one additional hour. The reaction mixture was poured into EtOAc (500 mL) and washed with H_2O400 mL. The organic phase was dried over Na_2SO_4 and concentrated in vacuo. The crude material was purified by column chromatography (SiO_2, EtOAc/Heptane 1:1) to give ethyl 4,6- dimethylpyrazolo[1,5-a]pyrazine-2-carboxylate **9-a** (5.01 g, 82%) as a yellow solid. ^{1}H NMR (600 MHz, DMSO-*d*6) δ ppm: 8.54 (d, *J*=0.7 Hz, 1H), 7.48 (d, *J*=1.0 Hz, 1H), 4.36 (q, *J*=7.1 Hz, 2H), 2.65 - 2.73 (m, 3H), 2.42 (d, *J*=0.9 Hz, 3H), 1.34 (t, *J*=7.1 Hz, 3H); LC-HRMS: m/z=219.10176 [(M+H)+ calcd for $C_{11}H_{13}N_3O_2$: 219.10078; Diff 1 mDa].

Step D. Preparation of **10-a**. A solution of ethyl 4,6-dimethylpyrazolo[1,5-a]pyrazine-2-carboxylate **9-a** (25.12 g, 115 mmol)and EtOAc (50.5 g, 56.1 mL, 575 mmol) in THF (1.50 L) was cooled down to -40 °C. LiHMDS (286 mL, 1M in THF/Ethylbenzene, 286 mmol) was slowly added over 1 hour and stirring was continued for one additional hour at -40 °C (dark solution). The reaction was quenched by addition of an aqueous saturated NH_4Cl solution (200 mL). The reaction mixture was concentrated in vacuo, poured into EtOAc and then washed several times with water. The organic phase was dried over Na_2SO_4, and concentrated in vacuo. The residue was purified by column chromatography (SiO_2, CH_2Cl_2/EtOAc 9:1 to 8:2) to give ethyl 3-(4,6-dimethylpyrazolo[1,5-a]pyrazin-2-yl)-3-oxo-propanoate **10-a** (23.02 g, 77%) as a yellow solid.

Step E. Preparation of **11-a**. A mixture of ethyl 3-(4,6-dimethylpyrazolo [1,5-a]pyrazin-2-yl)-3-oxo-propanoate **10-a** (261 mg, 1.0 mmol), 2-amino-5-fluoropyridine (134 mg, 1.2 mmol)

and PPTS (12.6 mg, 0.05 mmol) was heated at 130 °C. After 8 hours, the mixture was cooled to RT, concentrated in vacuo and chromatographed (SiO_2, EtOAc) to give 2-(4,6-dimethylpyrazolo[1,5-a]pyrazin-2-yl)-7-fluoro-pyrido[1,2-a]pyrimidin-4-one **11-a** (220 mg, 71%) as a yellow solid.

Step F. A solution of 2-(4,6-dimethylpyrazolo[1,5-a]pyrazin-2-yl)-7-fluoro-pyrido[1,2-a]pyrimidin-4-one **11-a** (309 mg, 1.0 mmol) and 1-methylpiperazine (1.1 mL, 10 mmol) in DMA (1.0 mL) was heated at 120 °C. After 15 h, the volatiles were removed and the residue was washed with CH_3CN to give 2-(4,6-dimethylpyrazolo[1,5-a]pyrazin-2-yl)-7-(4-methylpiperazin-1-yl)pyrido[1,2-a]pyrimidin-4-one **12** (313 mg, 80%) as a yellow solid. ^{1}H NMR (600 MHz, DMSO-*d*6) δ ppm: 8.55 (s, 1H), 8.27 (d, *J*=2.7 Hz, 1H), 8.11 (dd, *J*=9.7, 2.8 Hz, 1H), 7.71 (d, *J*=9.7 Hz, 1H), 7.53 (d, *J*=0.9 Hz, 1H), 6.95 (s, 1H), 3.26 (br s, 4H), 2.73 (s, 3H), 2.52 - 2.62 (m, 4H), 2.43 (d, *J*=0.6 Hz, 3H), 2.28 (br s, 3H); LC-HRMS: m/z=389.19807 [(M+H)+ calcd for $C_{21}H_{23}N_7O$: 389.19641; Diff 1.7 mDa].

7-[(8aS)-3,4,6,7,8,8a-Hexahydro-1H-pyrrolo[1,2-a]pyrazin-2-yl]-2-(4-ethyl-6-methyl-pyrazolo[1,5-a]pyrazin-2-yl)pyrido[1,2-a]pyrimidin-4-one (**13**). According to scheme 1: *Step E*. Preparation of **11-b**. With a similar procedure as for the preparation of **11-a**, upon reaction of ethyl 3-(4-ethyl-6-methyl-pyrazolo[1,5-a]pyrazin-2-yl)-3-oxo-propanoate **10-b** (2 g, 7.26 mmol) and 2-amino-5-fluoro-pyridine (0.98 g, 8.72 mmol) was obtained 2-(4-ethyl-6-methyl-pyrazolo[1,5-a]pyrazin-2-yl)-7-fluoro-pyrido[1,2-a]pyrimidin-4-one **11-b** (2.01 g, 86%) as an off-white solid. ^{1}H NMR (600 MHz, DMSO-*d*6) δ ppm: 8.97 (dd, *J*=4.7, 2.9 Hz, 1H), 8.56 (s, 1H), 8.15 (ddd, *J*=9.8, 7.1, 2.9 Hz, 1H), 7.88 (dd, *J*=9.8, 5.3 Hz, 1H), 7.59 (d, *J*=0.9 Hz, 1H),

7.04 (s, 1H), 3.09 (q, *J*=7.6 Hz, 2H), 2.45 (d, *J*=0.8 Hz, 3H), 1.34 (t, *J*=7.6 Hz, 3H); LC-HRMS: m/z=323.1198 [(M+H)+ calcd for $C_{17}H_{14}FN_5O$: 323.11824; Diff 1.6 mDa].

Step G. A solution of 2-(4-ethyl-6-methyl-pyrazolo[1,5-a]pyrazin-2-yl)-7-fluoro-pyrido [1,2-a]pyrimidin-4-one **11-b** (6.0 g, 18.6 mmol), (8aS)-1,2,3,4,6,7,8,8a-octahydropyrrolo[1,2-a]pyrazine (4.69 g, 37.2 mmol) and K_2CO_3 (2.56 g, 18.6 mmol) in DMSO (186 mL) was heated at 110 °C for 48 hours. The reaction was cooled down to RT, concentrated in vacuo and chromatographed (SiO_2, CH_2Cl_2/MeOH 95:5) to give 7-[(8aS)-3,4,6,7,8,8a-hexahydro-1H-pyrrolo[1,2-a]pyrazin-2-yl]-2-(4-ethyl-6-methyl-pyrazolo[1,5-a]pyrazin-2-yl)pyrido[1,2-a] pyrimidin-4-one **13** (5.0 g, 63%) as a yellow solid. ^{1}H NMR (600 MHz, CHLOROFORM-d) δ ppm: 8.49 (d, *J*=2.4 Hz, 1H), 8.15 (s, 1H), 7.74 – 7.79 (m, 1H), 7.68 – 7.74 (m, 1H), 7.36 (d, *J*=1.0 Hz, 1H), 7.17 (s, 1H), 3.79 – 3.83 (m, 1H), 3.61 – 3.87 (m, 1H), 3.15 – 3.20 (m, 1H), 3.13 – 3.32 (m, 1H), 3.04 (br s, 1H), 3.10 (d, *J*=7.7 Hz, 2H), 2.67 (br s, 1H), 2.53 (d, *J*=0.8 Hz, 3H), 2.43 (br s, 1H), 2.20 - 2.26 (m, 1H), 2.18 – 2.22 (m, 1H), 1.91 - 1.97 (m, 1H), 1.93 (br s, 1H), 1.82 (br s, 1H), 1.52 - 1.55 (m, 1H), 1.44 (t, *J*=7.6 Hz, 3H); LC-HRMS: m/z=429.22881 [(M+H)+ calcd for $C_{24}H_{27}N_7O$: 429.22771; Diff 1.1 mDa].

2-(4,6-Dimethylpyrazolo[1,5-a]pyrazin-2-yl)-9-methyl-7-(4-piperidyl)pyrido[1,2-a]pyrimidin-4-one (**15**). According to scheme 1. *Step H*. With a similar procedure as for the preparation of **16** (herein above), upon reaction of ethyl 3-(4,6-dimethylpyrazolo[1,5-a]pyrazin-2-yl)-3-oxo-propanoate **10-a** (4.97 g, 19.0 mmol) and tert-butyl 4-(6-amino-5-methyl-3-pyridyl)piperidine-1-carboxylate **14** (5.54 g, 19.0 mmol) was obtained the title product **15** (2.85 g, 39%) as a yellow solid. ^{1}H NMR (600 MHz, CHLOROFORM-d) δ ppm: 8.85 (d, *J*=1.7 Hz, 1H), 8.13 (d, *J*=0.6 Hz, 1H), 7.58 (d, *J*=0.9 Hz, 1H), 7.45 (d, *J*=1.0 Hz, 1H), 7.27 (s, 1H), 3.26

(br d, *J*=12.1 Hz, 2H), 2.74 (br d, *J*=3.5 Hz, 4H), 2.67 - 2.85 (m, 5H), 2.53 (d, *J*=0.8 Hz, 3H), 1.89 - 1.96 (m, 2H), 1.72 (qd, *J*=12.4, 4.0 Hz, 2H); LC-HRMS: m/z=388.20194 [(M+H)+ calcd for $C_{22}H_{24}N_6O_2$: 388.20116; Diff 0.8 mDa].

2-(4,6-Dimethylpyrazolo[1,5-a]pyrazin-2-yl)-9-methyl-7-(1-methyl-4-piperidyl) pyrido[1,2-a]pyrimidin-4-one (**17**). According to scheme 1. *Step J*. With a similar procedure as for the preparation of **3**, upon reaction of 2-(4,6-dimethylpyrazolo[1,5-a]pyrazin-2-yl)-9-methyl-7-(4-piperidyl)pyrido[1,2-a]pyrimidin-4-one **15** (0.35 g, 0.90 mmol) and a formaldehyde solution (0.207 mL, 37 wt% in H_2O, 2.70 mmol) was obtained the title product **17** (0.17 g, 47%) as an off-white solid. ^{1}H NMR (600 MHz, DMSO-*d*6) δ ppm: 8.71 (s, 1H), 8.57 (s, 1H), 7.96 (s, 1H), 7.60 (d, *J*=0.9 Hz, 1H), 7.01 (s, 1H), 3.01 (br s, 2H), 2.75 (s, 3H), 2.70 (br d, *J*=10.2 Hz, 1H), 2.66 (s, 3H), 2.44 (s, 3H), 2.32 (br s, 3H), 2.09 - 2.26 (m, 1H), 2.19 (br s, 1H), 1.90 (br d, *J*=12.2 Hz, 2H), 1.71 - 1.80 (m, 2H); LC-HRMS: m/z=402.21824 [(M+H)+ calcd for $C_{23}H_{26}N_6O$: 402.21681; Diff 1.4 mDa].

2-(4,6-Dimethylpyrazolo[1,5-a]pyrazin-2-yl)-7-(1-ethyl-4-piperidyl)-9-methyl-pyrido[1,2-a]pyrimidin-4-one (**18**). According to scheme 1. *Step J*. With a similar procedure as for the preparation of **17**, upon reaction of 2-(4,6-dimethylpyrazolo[1,5-a]pyrazin-2-yl)-9-methyl-7-(4-piperidyl)pyrido[1,2-a]pyrimidin-4-one **15** (2.80 g, 7.21 mmol) and an acetaldehyde solution (21.6 mL, 1 M in EtOH, 21.6 mmol) was obtained the title product **18** (2.71 g, 90%) as an off-white solid. ^{1}H NMR (600 MHz, DMSO-*d*6) δ ppm: 8.69 (s, 1H), 8.56 (s, 1H), 7.96 (s, 1H), 7.57 (d, *J*=0.9 Hz, 1H), 6.99 (s, 1H), 3.09 (br s, 2H), 2.73 - 2.77 (m, 3H), 2.69 - 2.74 (m, 1H), 2.65 (s, 3H), 2.29 - 2.47 (m, 5H), 1.94 - 2.27 (m, 2H), 1.85 - 1.94 (m, 2H), 1.72 (br d,

J=10.6 Hz, 2H), 1.06 (br t, *J*=6.9 Hz, 3H); LC-HRMS: m/z=416.23381 [(M+H)+ calcd for $C_{24}H_{28}N_6O$: 416.23246; Diff 1.4 mDa].

2-(4-Ethyl-6-methyl-pyrazolo[1,5-a]pyrazin-2-yl)-9-methyl-7-(1,2,3,6-tetrahydro-pyridin-4-yl)pyrido[1,2-a]pyrimidin-4-one (**20**). According to scheme 1. *Step I*. With a similar procedure as for the preparation of **16**, upon reaction of ethyl 3-(4-ethyl-6-methyl-pyrazolo[1,5-a]pyrazin-2-yl)-3-oxo-propanoate **10-b** (6.80 g, 24.7 mmol) and tert-butyl 4-(6-amino-5-methyl-3-pyridyl)-3,6-dihydro-2H-pyridine-1-carboxylate (7.86 g, 27.2 mmol) was obtained the title product **20** (3.15 g, 32%) as an off-white solid. ^{1}H NMR (600 MHz, DMSO-*d*6) δ ppm: 8.70 (s, 1H), 8.53 (s, 1H), 8.16 (s, 1H), 7.55 (s, 1H), 6.98 (s, 1H), 6.56 (br s, 1H), 3.49 (br s, 2H), 3.09 (q, *J*=7.5 Hz, 2H), 3.01 (br t, *J*=5.1 Hz, 2H), 2.65 (s, 3H), 2.42 - 2.46 (m, 2H), 2.39 - 2.45 (m, 3H), 1.34 (t, *J*=7.5 Hz, 3H); LC-HRMS: m/z=400.2023 [(M+H)+ calcd for $C_{23}H_{24}N_6O$: 400.20116; Diff 1.1 mDa].

2-(1-Methylbenzimidazol-5-yl)-7-(4-methylpiperazin-1-yl)pyrido[1,2-a]pyrimidin-4-one (**24**). According to scheme 2: With a similar procedure as for the preparation of **4**, from 2-chloro-7-fluoro-pyrido[1,2-a]pyrimidin-4-one **22** (0.25 g, 1.26 mmol) and (1-methyl benzimidazol-5-yl)boronic acid (0.33 g, 1.89 mmol) was obtained 7-fluoro-2-(1-methyl benzimidazol-5-yl)pyrido[1,2-a]pyrimidin-4-one **23-a** (0.26 g, 70%). Further reaction with 1-methylpiperazine (0.40 mL, 3.66 mmol) gave 2-(1-methylbenzimidazol-5-yl)-7-(4-methylpiperazin-1-yl)pyrido[1,2-a]pyrimidin-4-one **24** (0.19 g, 54%) as a yellow solid. ^{1}H NMR (600 MHz, DMSO-*d*6) δ ppm: 8.44 (d, *J*=1.3 Hz, 1H), 8.29 (s, 1H), 8.26 (d, *J*=2.7 Hz, 1H), 8.09 - 8.12 (m, 1H), 8.08 (br d, *J*=2.7 Hz, 1H), 7.73 - 7.76 (m, 1H), 7.72 (s, 1H), 7.07 (s, 1H), 3.93 (s,

3 H), 3.25 (br s, 4H), 2.52 - 2.62 (m, 4H), 2.28 (br s, 3H); LC-HRMS: m/z=375.1928 [(M+H)+ calcd for $C_{21}H_{22}N_6O$: 375.1928; Diff 0 mDa].

7-(4-Methylpiperazin-1-yl)-2-(2-methyl-[1,2,4]triazolo[1,5-a]pyridin-6-yl)pyrido[1,2-a]pyrimidin-4-one (**25**). According to scheme 2: With a similar procedure as for the preparation of **4**, from 2-chloro-7-fluoro-pyrido[1,2-a]pyrimidin-4-one **22** (0.52 g, 2.61 mmol) and 6-bromo-2-methyl-[1,2,4]triazolo[1,5-a]pyridine (0.81 g, 3.71 mmol) was obtained 7-fluoro-2-(2-methyl-[1,2,4]triazolo[1,5-a]pyridin-6-yl)pyrido[1,2-a]pyrimidin-4-one **23-b** (0.27 g, 31%). Further reaction with 1-methylpiperazine (0.30 mL, 2.74 mmol) gave 7-(4-methylpiperazin-1-yl)-2-(2-methyl-[1,2,4]triazolo[1,5-a]pyridin-6-yl)pyrido[1,2-a]pyrimidin-4-one **25** (216 mg, 63%) as a yellow solid. ^{1}H NMR (600 MHz, DMSO-*d*6) δ ppm: 9.60 (s, 1H), 8.41 (dd, *J*=9.4, 1.7 Hz, 1H), 8.26 (d, *J*=2.6 Hz, 1H), 8.14 (dd, *J*=9.6, 2.6 Hz, 1H), 7.79 - 7.85 (m, 1H), 7.76 (d, *J*=9.7 Hz, 1H), 7.14 (s, 1H), 3.26 (overlapped with water, 4H), 2.51 (overlapped with DMSO-d6, 7H), 2.25 (s, 3 H); LC-HRMS: m/z=375.18275 [(M+H)+ calcd for $C_{20}H_{21}N_7O$: 375.18076; Diff 2 mDa].

2-(2-Methyl-1,3-benzoxazol-6-yl)-7-(4-methylpiperazin-1-yl)pyrido[1,2-a]pyrimidin-4-one (**26**). According to scheme 2: With a similar procedure as for the preparation of **4**, from 2-chloro-7-fluoro-pyrido[1,2-a]pyrimidin-4-one **22** (0.25 g, 1.26 mmol) and (2-methyl-1,3-benzoxazol-6-yl)boronic acid (0.33 g, 1.89 mmol) was obtained 7-fluoro-2-(2-methyl-1,3-benzoxazol-6-yl)pyrido[1,2-a]pyrimidin-4-one **23-c** (0.36 g, 97%). Further reaction with 1-methylpiperazine (0.41 mL, 3.67 mmol) gave 2-(2-methyl-1,3-benzoxazol-6-yl)-7-(4-methylpiperazin-1-yl)pyrido[1,2-a]pyrimidin-4-one **26** (0.17 g, 38%) as a yellow solid. ^{1}H NMR (600 MHz, DMSO-*d*6) δ ppm: 8.47 (d, *J*=1.5 Hz, 1H), 8.26 (s, 1H), 8.23 (d, *J*=8.5 Hz, 1H), 8.11

(dd, *J*=9.7, 2.8 Hz, 1H), 7.75 (t, *J*=9.3 Hz, 2H), 7.05 (s, 1H), 3.20 - 3.29 (m, 4H), 2.66 (s, 3H), 2.52 - 2.63 (m, 4H), 2.29 (br s, 3H); LC-HRMS: m/z=375.17126 [(M+H)+ calcd for $C_{21}H_{21}N_5O_2$: 375.16952; Diff 1.7 mDa].

2-(4-Fluoro-2-methyl-1,3-benzoxazol-6-yl)-7-(4-methylpiperazin-1-yl)pyrido[1,2-a]pyrimidin-4-one (**27**). According to scheme 2: With a similar procedure as for the preparation of **4**, from 2-chloro-7-fluoro-pyrido[1,2-a]pyrimidin-4-one **22** (1.16 g, 5.85 mmol) and 6-bromo-4-fluoro-2-methyl-1,3-benzoxazole (1.57 g, 6.82 mmol) was obtained 7-fluoro-2-(4-fluoro-2-methyl-1,3-benzoxazol-6-yl)pyrido[1,2-a]pyrimidin-4-one **23-d** (1.53 g, 75%). Further reaction with 1-methylpiperazine (1.19 mL, 10.7 mmol) gave 2-(4-fluoro-2-methyl-1,3-benzoxazol-6-yl)-7-(4-methylpiperazin-1-yl)pyrido[1,2-a]pyrimidin-4-one **27** (0.88 g, 46%) as a yellow solid. ^{1}H NMR (600 MHz, DMSO-*d*6) δ ppm: 8.38 (d, *J*=1.2 Hz, 1H), 8.24 (d, *J*=2.7 Hz, 1H), 8.10 - 8.14 (m, 1H), 8.07 - 8.11 (m, 1H), 7.74 (d, *J*=9.7 Hz, 1H), 7.11 (s, 1H), 3.23 - 3.29 (m, 4H), 2.68 (s, 3H), 2.51 - 2.57 (m, 4H), 2.27 (s, 3H); LC-HRMS: m/z=393.16167 [(M+H)+ calcd for $C_{21}H_{20}F N_5O_2$: 393.1601; Diff 1.6 mDa].

Preparation of 6-bromo-4-fluoro-2-methyl-1,3-benzoxazole: A mixture of 2-amino-5-bromo-3-fluorophenol (2.1 g, 10.2 mmol), 1,1,1-triethoxyethane (9.4 mL, 51.0 mmol)and TFA (0.785 mL, 10.2 mmol) were stirred at RT for 24 hours. The reaction was diluted in EtOAc and H_2O and solid Na_2CO_3 until the pH of the aqueous phase reached 10. The organic phase was dried over Na_2SO_4, concentrated in vacuo and column chromatography (SiO_2, EtOAc/Heptane 1:6 to 1/4) gave 6-bromo-4-fluoro-2-methyl-1,3-benzoxazole (2.10 g, 76%) as a white solid.

2-(4-Fluoro-2-methyl-1,3-benzoxazol-6-yl)-7-piperazin-1-yl-pyrido[1,2-a]pyrimidin-4-one (**28**). According to scheme 2: With a similar procedure as for the preparation of **4**, from 7-fluoro-2-(4-fluoro-2-methyl-1,3-benzoxazol-6-yl)pyrido[1,2-a]pyrimidin-4-one **23-d** (0.40 g, 1.28 mmol) and piperazine (0.33 g, 3.83 mmol) was obtained the title compound **28** (0.32 g, 66%) as a yellow solid. ^{1}H NMR (600 MHz, DMSO-*d*6) δ ppm: 8.38 (d, *J*=1.3 Hz, 1H), 8.24 (d, *J*=2.6 Hz, 1H), 8.09 - 8.12 (m, 1H), 8.08 - 8.12 (m, 1H), 7.75 (d, *J*=9.7 Hz, 1H), 7.12 (s, 1H), 3.16 - 3.25 (m, 4H), 2.95 - 3.00 (m, 4H), 2.68 (s, 3H); LC-HRMS: m/z=380.15127 [(M+H)+ calcd for $C_{20}H_{19}FN_5O_2$: 380.152278098; Diff -1 mDa].

2-Imidazo[1,2-a]pyridin-6-yl-7-(4-methylpiperazin-1-yl)pyrido[1,2-a]pyrimidin-4-one (**29**). According to scheme 2: With a similar procedure as for the preparation of **4**, from 2-chloro-7-fluoro-pyrido[1,2-a]pyrimidin-4-one **22** (0.25 g, 1.26 mmol) and 6-bromoimidazo[1,2-a]pyridine (0.40 g, 2.03 mmol) was obtained 7-fluoro-2-imidazo[1,2-a]pyridin-6-yl-pyrido[1,2-a]pyrimidin-4-one **23-e**. Further reaction with 1-methylpiperazine (0.24 mL, 2.14 mmol) gave 2-imidazo[1,2-a]pyridin-6-yl-7-(4-methylpiperazin-1-yl)pyrido[1,2-a]pyrimidin-4-one **29** (0.11 g, 25% overall yield) as a yellow solid. ^{1}H NMR (600 MHz, DMSO-*d*6) δ ppm: 9.45 (dd, *J*=1.7, 0.9 Hz, 1H), 8.25 (d, *J*=2.7 Hz, 1H), 8.11 (dd, *J*=9.7, 2.8 Hz, 1H), 8.08 (s, 1H), 7.99 (dd, *J*=9.6, 1.8 Hz, 1H), 7.70 (d, *J*=9.7 Hz, 1H), 7.63 - 7.68 (m, 1H), 7.63 - 7.66 (m, 1H), 6.97 (s, 1H), 3.25 (br s, 4H), 2.54 (br s, 4H), 2.27 (s, 3H); LC-HRMS: m/z=360.17272 [(M+H)+ calcd for $C_{20}H_{20}N_6O$: 360.16986; Diff 2.9 mDa].

2-(2-Methylimidazo[1,2-a]pyridin-6-yl)-7-(4-methylpiperazin-1-yl)pyrido[1,2-a]pyrimidin-4-one (**30**). According to scheme 2: With a similar procedure as for the preparation

of **4**, from 2-chloro-7-fluoro-pyrido[1,2-a]pyrimidin-4-one **22** (0.25 g, 1.26 mmol) and (2-methylimidazo[1,2-a]pyridin-6-yl)boronic acid (0.33 g, 1.89 mmol) was obtained 7-fluoro-2-(2-methylimidazo[1,2-a]pyridin-6-yl)pyrido[1,2-a]pyrimidin-4-one **23-f** (0.32 g, 79%). Further reaction with 1-methylpiperazine (0.37 mL, 3.31 mmol) gave 2-(2-methylimidazo[1,2-a]pyridin-6-yl)-7-(4-methylpiperazin-1-yl)pyrido[1,2-a]pyrimidin-4-one **30** (0.13 g, 31%) as a yellow solid. ^{1}H NMR (600 MHz, DMSO-*d*6) δ ppm: 9.35 (dd, *J*=1.7, 0.9 Hz, 1H), 8.26 (d, *J*=2.7 Hz, 1H), 8.11 (dd, *J*=9.7, 2.8 Hz, 1H), 7.94 (dd, *J*=9.5, 1.8 Hz, 1H), 7.81 (s, 1H), 7.70 (d, *J*=9.7 Hz, 1H), 7.52 (d, *J*=9.4 Hz, 1H), 6.96 (s, 1H), 3.18 - 3.29 (m, 4H), 2.53 - 2.67 (m, 4H), 2.36 (d, *J*=0.6 Hz, 3H), 2.31 (br s, 3H); LC-HRMS: m/z=374.18788 [(M+H)+ calcd for $C_{21}H_{22}N_6O$: 374.18551; Diff 2.4 mDa].

2-(8-Fluoro-2-methyl-imidazo[1,2-a]pyridin-6-yl)-7-piperazin-1-yl-pyrido[1,2-a]pyrimidin-4-one (**31**). According to scheme 2: With a similar procedure as for the preparation of **4**, from 7-fluoro-2-(8-fluoro-2-methyl-imidazo[1,2-a]pyridin-6-yl)pyrido[1,2-a]pyrimidin-4-one **23-h** (0.71 g, 2.29 mmol) and piperazine (0.59 g, 6.87 mmol) was obtained the title compound **31** (0.47 g, 55%) as a yellow solid. ^{1}H NMR (600 MHz, DMSO-*d*6) δ ppm: 9.24 - 9.28 (m, 1H), 8.21 - 8.26 (m, 1H), 8.08 - 8.14 (m, 1H), 7.93 (d, *J*=2.3 Hz, 1H), 7.84 - 7.89 (m, 1H), 7.70 (d, *J*=9.7 Hz, 1H), 6.97 - 7.01 (m, 1H), 3.20 - 3.25 (m, 4H), 2.95 - 3.02 (m, 4H), 2.38 (s, 3H); LC-HRMS: m/z=378.15906 [(M+H)+ calcd for $C_{20}H_{19}FN_6O$: 378.160437488; Diff -1.4 mDa].

2-[2-Methyl-8-(trifluoromethyl)imidazo[1,2-a]pyridin-6-yl]-7-(4-pyrrolidin-1-yl-1-piperidyl)pyrido[1,2-a]pyrimidin-4-one (**40**). With a similar procedure as for the preparation of

4, from 2-chloro-7-fluoro-pyrido[1,2-a]pyrimidin-4-one **22** (1.15 g, 5.79 mmol) and 6-bromo-2-methyl-8-(trifluoromethyl)imidazo[1,2-a]pyridine (2.00 g, 7.17 mmol) was obtained 7-fluoro-2-[2-methyl-8-(trifluoromethyl)imidazo[1,2-a]pyridin-6-yl]pyrido[1,2-a]pyrimidin-4-one (2.10 g, 91%). Further reaction of [2-methyl-8-(trifluoromethyl)imidazo[1,2-a]pyridin-6-yl]pyrido[1,2-a]pyrimidin-4-one (0.17 g, 0.469 mmol) with 4-pyrrolidin-1-ylpiperidine (0.21 g, 1.38 mmol) in the presence of Et_3N (0.26 mL, 1.88 mmol) in DMSO (5 mL) at 110 °C gave after column chromatography (SiO_2, CH_2Cl_2/MeOH 98:2 to 9:1) 2-[2-methyl-8-(trifluoromethyl)imidazo[1,2-a]pyridin-6-yl]-7-(4-pyrrolidin-1-yl-1-piperidyl)pyrido[1,2-a] pyrimidin-4-one **40** (0.11 g, 46%) as a yellow solid. ^{1}H NMR (600 MHz, CHLOROFORM-d) δ ppm: 9.08 (s, 1H), 8.44 (d, *J*=2.7 Hz, 1H), 8.13 (s, 1H), 7.70 - 7.76 (m, 1H), 7.63 - 7.69 (m, 1H), 7.55 (s, 1H), 6.81 (s, 1H), 3.76 (br d, *J*=10.3 Hz, 2H), 2.30 - 3.37 (m, 10H), 1.63 - 2.29 (m, 6H); LC-HRMS: m/z=496.22077 [(M+H)+ calcd for $C_{26}H_{27}F_3N_6O$: 496.21984; Diff 0.9 mDa].

Preparation of 6-bromo-2-methyl-8-(trifluoromethyl)imidazo[1,2-a]pyridine: A solution of 5-bromo-3-(trifluoromethyl)pyridin-2-amine (2.5 g, 10.4 mmol), 1-bromo-2,2-dimethoxypropane (1.57 mL, 11.4 mmol) and PPTS (0.27 g, 1.04 mmol) in 2-propanol (25 mL) was heated at reflux for 12 hours. The reaction was cooled down to RT and the volatiles were removed in vacuo. The residue was dissolved in EtOAc (100 mL) then washed with aqueous $NaHCO_3$. The organic phase was dried over Na_2SO_4, concentrated in vacuo to give 6-bromo-2-methyl-8-(trifluoromethyl)imidazo[1,2-a]pyridine (2.10 g, 96%) as a white solid.

7-[4-(Azetidin-1-yl)-1-piperidyl]-2-(1,3-dimethylpyrrolo[1,2-a]pyrazin-7-yl)pyrido [1,2-a]pyrimidin-4-one (**41**). *Step 1*: To a solution of 2,3,5-trimethylpyrazine (10.00 g, 65.5 mmol) in CH_3CN (115 mL) was added ethyl 3-bromo-2-oxopropanoate (90%, 9.15 mL, 65.5

mmol) and the reaction mixture was heated at reflux for 3 days. Triethyl amine (27.4 mL, 196 mmol) was added at RT and the reaction mixture was stirred at 60 °C for 2 h. The reaction was cooled down to RT, poured into H_2O, the product was extracted with EtOAc, and the organic phase was dried over Na_2SO_4 and evaporated. Column chromatography (SiO_2, EtOAc/Heptane 1:1) gave ethyl 1,3-dimethylpyrrolo[1,2-a]pyrazine-7-carboxylate (8.03 g, 56%) as an off-white solid.

Step 2. To a solution of ethyl 1,3-dimethylpyrrolo[1,2-a]pyrazine-7-carboxylate (2.86 g, 13.1 mmol) in THF (46 mL) was added t-butyl acetate (4.25 mL, 31.4 mmol) and the reaction mixture was cooled to -75 °C. LiHMDS (31.4 mL, 1 M in THF, 31.4 mmol) was added dropwise at -75 °C. The temperature was raised to RT over one hour, and the reaction mixture was quenched by addition of an aqueous saturated NH_4Cl solution (50 mL). The reaction mixture was poured into EtOAc and washed with water. The organic phase was dried over Na_2SO_4 and concentrated in vacuo. The residue was purified by chromatography (SiO_2, EtOAc/Heptane 1:1) to give tert-butyl 3-(1,3-dimethylpyrrolo[1,2-a]pyrazin-7-yl)-3-oxo-propanoate (3.27 g, 86%) as a light brown solid.

Step 3. A suspension of tert-butyl 3-(1,3-dimethylpyrrolo[1,2-a]pyrazin-7-yl)-3-oxo-propanoate (1.00 g, 3.47 mmol), 5-fluoropyridin-2-amine (0.467 g, 4.17 mmol) and PPTS (0.872 g, 3.47 mmol) in 3-methyl-1-butanol (10 mL) was heated at reflux for 16 h. The brown suspension was cooled to RT and heptane (10 mL) was added. The solid was recovered by filtration, washed several times with heptane and dried under in to give 2-(1,3-dimethylpyrrolo[1,2-a]pyrazin-7-yl)-7-fluoro-pyrido[1,2-a]pyrimidin-4-one (1.12 g, 67%).

Step 4. A mixture of 2-(1,3-dimethylpyrrolo[1,2-a]pyrazin-7-yl)-7-fluoro-pyrido[1,2-a]pyrimidin-4-one (0.500 g, 1.04 mmol), 1,4-dioxa-8-azaspiro[4.5]decane (0.267 mL, 2.08

mmol) and K_2CO_3 (0.575 g, 4.16 mmol) in DMA (3.2 mL) was stirred in a sealed tube at 120 °C for 24 h. The reaction was cooled to RT, diluted with EtOAC, and washed with H_2O. The organic phase was dried over Na_2SO_4 and concentrated in vacuo. The residue was suspended in dioxane (5 mL) and HCl (4.7 mL, 6N) was added. After one hour, the reaction was poured slowly into an aqueous saturated solution of $NaHCO_3$ and the product extracted with EtOAc. The organic phase was dried over Na_2SO_4, concentrated in vacuo and chromatographed (SiO_2, CH_2Cl_2/MeOH 98:2 to 9:1) to give 2-(1,3-dimethylpyrrolo[1,2-a]pyrazin-7-yl)-7-(4-oxo-1-piperidyl)pyrido[1,2-a]pyrimidin-4-one (0.25 g, 60%) as a yellow solid.

Step 5. To a suspension of 2-(1,3-dimethylpyrrolo[1,2-a]pyrazin-7-yl)-7-(4-oxo-1-piperidyl)pyrido[1,2-a]pyrimidin-4-one (100 mg, 0.26 mmol) and azidine (18 mg, 0.31 mmol) in CH_2Cl_2 (2.3 mL) was added AcOH (~ 0.020 mL, to set pH ~ 5). Sodium triacetoxyborohydride (115 mg, 0.54 mmol) was added portion wise keeping the temperature below 28 °C and stirring was continued at RT for an additional 2 hours. The reaction mixture was diluted with CH_2Cl_2 and washed with an aqueous $NaHCO_3$ solution. The organic phase was dried over Na_2SO_4, concentrated and chromatographed (SiO_2, CH_2Cl_2/MeOH 98:2 to 9:1) to give 7-[4-(azetidin-1-yl)-1-piperidyl]-2-(1,3-dimethylpyrrolo[1,2-a]pyrazin-7-yl)pyrido[1,2-a] pyrimidin-4-one **41** (102 mg, 92%) as a yellow solid. ^{1}H NMR (600 MHz, DMSO-*d*6) δ ppm: 8.25 (d, *J*=1.4 Hz, 1H), 8.24 (d, *J*=2.7 Hz, 1H), 8.04 (dd, *J*=9.7, 2.8 Hz, 1H), 7.96 (s, 1H), 7.61 (d, *J*=9.7 Hz, 1H), 7.42 (s, 1H), 6.84 (s, 1H), 3.60 (br d, *J*=11.4 Hz, 2H), 3.14 - 3.29 (m, 4H), 2.79 - 2.91 (m, 2H), 2.58 (s, 3H), 2.28 (s, 3H), 1.99 (br s, 2H), 1.79 (br d, *J*=9.4 Hz, 2H), 1.33 (q, *J*=9.3 Hz, 2H); LC-HRMS: m/z=428.23113 [(M+H)+ calcd for $C_{25}H_{28}N_6O$: 428.23246; Diff -1.3 mDa].

Ames mutagenicity test

The profiling of test compounds for their mutagenic potential was performed using an AMES bacterial reverse mutation test essentially as described previously. In brief, Salmonella typhimurium strains TA1535, TA97, TA98, TA100, and TA102 were obtained from B. N. Ames (University of California, Berkeley, USA). S9 rat liver mixtures were freshly prepared for each experiment by mixing 0.1 mL of S9 preparation (Molecular Toxicology Inc., Boone, NC, USA), 0.2 mL of a 165 mM KCl solution, 0.2 mL of a 40 mM MgCl2 solution, 0.2 mL of 200 mM sodium phosphate buffered saline, pH 7.4, 3.2 mg of NADP (Roche Diagnostics, Rotkreuz, Switzerland), and 1.53 mg of glucose 6-phosphate (Roche Diagnostics). Bacterial growth media and agar, supplements, and tetracycline were obtained from Sigma (Buchs, Switzerland). Cultures of the strains were grown overnight at 37°C in a shaking water bath in a nutrient broth (NB) liquid medium to which 0.3 μg/mL tetracycline was added for strain TA102 in order to maintain a stable plasmid copy number. The bacterial density was checked photometrically, and cultures were diluted in 0.85% NaCl as needed. The sensitivity of the Salmonella typhimurium strains was verified using the following positive controls: NaN_3 with strains TA1535 and TA100, ICR 191 with strain TA97, 2-nitrofluorene with strain TA98, and MMC with strain TA102. Moreover, 2-aminoanthracene was used with all strains, with and without metabolic activation, to confirm the activity of the S9 mix. For testing of compounds, test tubes containing 2 mL of 0.7% agar medium were autoclaved and kept in a prewarmed water bath at 42−45 °C, and the following solutions were added: (a) 0.2 mL of a histidine/biotin mixture corresponding to 21 μg of L-histidine and 24.4 μg of biotin, (b) 0.1 mL solutions of test compound (20−2000 μg/ plate) and positive controls, (c) 0.1 mL of bacterial overnight liquid cultures, (d) 0.5 mL of the S9 mixture where metabolic activation was needed, or 0.5 mL of 200 mM sodium phosphate buffered saline, pH 7.4, where no metabolic activation was needed. The contents of the tubes

were mixed and poured immediately onto Vogel−Bonner minimal agar plates, allowed to solidify, and incubated at 37 °C upside down for 2 days. Bacterial colonies were counted electronically using a DOMINO automatic image analysis system (Perceptive Instruments, Haverhill, U.K.) after inspection of the background lawn for signs of toxicity. The outcome of the test was considered a positive result indicating mutagenicity when a dose dependent increase in the number of colonies was observed reaching at least a 2-fold (strains TA1535, TA98) or 1.5-fold (strains TA97, TA100, TA102) increase over the background level.

Lipophilicity (log D) determination by high-throughput shake-flask

The applied methods called CAMDIS© (**CA**rrier **M**ediated **DI**stribution **S**ystem) for the determination of distribution coefficients are derived from the conventional 'shake flask' method. CAMDIS© is carried out in 96-well microtiterplates in combination with the novel DIFI©-tubes constructed by Roche, which provide a hydrophobic layer for the octanol phase. The experiment starts with the accurate coating of the hydrophobic layer (0.45 mm PVDF membranes), which is fixed on the bottom of each DIFI©-tube: Each membrane is impregnated with exactly 1.0 mL 1-octanol by a robotic system (Microfluidic Dispenser BioRAPTR, Bechman Coulter). To expand the measurement range down to logD= -0.5, the procedure is carried at two different octanol/water ratios. One with a overplus of octanol for hydrophilic compounds (logD<1) and one with a low volume of octanol for the lipophilic compounds (logD>1). Therefore, some DIFI©-tubes are filled with 15 µl 1-octanol. The coated membranes are then connected to a 96-well plate which has been prefilled with exactly 150 mL of the selected aqueous buffer solution (25 mM Phosphate, pH 7.4). The buffer solution already contains the compound of interest with a starting concentration of 100 mM. The resulting

sandwich construct guarantees that the membrane is completely dipped in the buffered sample solution. The plate is then sealed and shaken for 24 hours at room temperature (23°C). During this time the substance is distributed between the layer, the octanol and the buffer solution. After distribution equilibrium is reached the DIFI©-tubes are easily disassembled from the top of the 96-well plate, so that the remaining sample concentration in the aqueous phase can be analyzed by LC/MS. In order to know the exact sample concentration before incubation with 1-octanol, a part of the sample solution is connected to DIFI©-tubes without impregnation. The distribution coefficient is then calculated from the difference in concentration in the aqueous phase with and without impregnation and the ratio of the two phases. The preparation of the sample solutions is carried out by a TECAN robotic system (RSP 100, 8 channels).

SMN HTRF assay

The levels of SMN protein in lysates of compound-treated cells were quantified as described previously.[7]

Pharmacokinetics, pharmacodynamics, and survival studies in mouse models

All studies were carried out in AAALAC-certified facilities and the protocols for animal experiments were approved by the Institutional Animal Care and Use Committee. All mice were maintained in specific pathogen-free conditions. Data were analyzed with GraphPad Prism software. The statistical significance of the EAE clinical scores between treatments was analyzed with a two-way ANOVA test (multiple comparisons vs vehicle).

Pharmacokinetic studies in animals: The pharmacokinetics of test compounds was evaluated in wild-type FVB mice. For oral dosing of adult mice, compounds were formulated as

a suspension in 0.5% hydroxypropylmethyl cellulose with 0.1% Tween 80 and administered at a dose of 10 mg/kg. For intraperitoneal dosing of 10-day old mice, compounds were formulated in DMSO and administered at a dosing volume of 2.5 mL/kg. After dosing, blood was collected by terminal cardiac puncture at specified time points (3 mice per time point), blood was centrifuged, and the plasma collected. The concentrations of test compound in plasma were quantified by liquid chromatography-tandem mass spectrometry (LC-MS/MS).

Pharmacodynamic studies in animals: To measure increases in SMN protein in vivo in adult C/C-allele mice (FVB.129(B6)-Smn1tm5(Smn1/SMN2)Mrph/J) animals were treated daily for 10 days. One hour after the tenth dose, mice were euthanized and the brain and quadriceps were collected. To measure increases in SMN protein in Δ7 mice, (([(FVB.Cg-Tg(SMN2*delta7) 4299Ahmb Tg(SMN2)89Ahmb Smn1tm1Msd/J) were dosed daily from PND3 through PND9. One hour after the last dose on PND9, mice were euthanized and the brain and quadriceps were collected. Tissue samples were collected, homogenized and transferred to a 96-well plate and were diluted in RIPA buffer. Samples were run in duplicate and averaged. SMN protein was quantified using Homogeneous Time Resolved Fluorescence (HTRF, Cisbio Bioassays) as previously published.[7] Total protein content was quantified in each tissue homogenate using the BCA assay according to the manufacturer's protocol. The HTRF signal for SMN protein was normalized to the total protein concentration for each sample generating the delta F SMN signal/ total protein. The percent increase was calculated as: 100 x (Treated – Vehicle)/Vehicle where the Vehicle is the mean SMN/total protein for the vehicle-dosed group and Treated is the SMN/total protein for each compound-dosed animal. Statistical differences between groups were determined using ANOVA (multiple comparisons vs vehicle; GraphPad, Carey NC).

Δ7 mouse survival studies: Homozygous Δ7 mice [(FVB.Cg-Tg(SMN2*delta7)4299Ahmb Tg(SMN2)89Ahmb Smn1tm1Msd/J were dosed IP with test compound or vehicle (100% DMSO; 2.5 mL/kg) once per day from PND3 through P23 and the dosing regimen was switched on P24 to a three-fold higher oral dose once daily in 0.5 % HPMC and 0.1% Tween 80. Litters were randomized across groups. Body weight and survival were assessed daily. Survival analysis was done using GraphPad Prism (Log-rank test) and a $p<0.05$ was considered as significant.

ASSOCIATE CONTENT

Supporting Information

Synthetic procedures for the preparation of compounds **33-37**, methods for RT-qPCR analysis of *SMN2* full length (FL) and Δ7 mRNAs in cultured cells, and motor function for compound **3**. This material is free of charge via the Internet at http://pubs.acs.org.

AUTHORS INFORMATION

Corresponding Authors

*Hasane Ratni. E-mail: hasane.ratni@roche.com; Phone: (+41) 61-688-2748. *Gary M. Karp. Email: gkarp@ptcbio.com; Phone: (+1) 908-912-9144.

ACKNOWLEDGMENTS

We thank Philippe Jablonski, Thierry Meyer, Barbara Mueller, Serge Burner, Virginie Brom, Anke Kurt and Heidi Schär for the synthesis of the compounds described, Josef Schneider for the NMR spectroscopy, Christian Bartelmus for the mass spectroscopy and Laura Gullett for correcting the manuscript. The research described in the manuscript was funded by F. Hoffmann-La Roche AG, PTC Therapeutics and the SMA Foundation.

ABBREVIATIONS USED

DMA, N,N-Dimethylacetamide ; DMAP, *N*,*N*-dimethylpyridin-4-amine; DMF, *N*,*N*-dimethylformamide; DMSO, dimethyl sulfoxide; Dppp, bis(diphenylphosphino)propane; i.p., intraperitoneal; NMR, nuclear magnetic resonance; P-gp, P-glycoprotein; PPTS, pyridinium p-toluenesulfonate; RT, room temperature; SMA, spinal muscular atrophy; SMN, survival of motor neuron; TFA, trifluoroacetic acid; THF, tetrahydrofuran.

REFERENCES

1. (a) Pearn, J. Classification of spinal muscular atrophies. *Lancet* **1980,** *1*, 919-922; (b) Crawford, T. O.; Pardo, C. A. The neurobiology of childhood spinal muscular atrophy. *Neurobiol. Dis.* **1996,** *3*, 97-110; (c) Sugarman, E. A.; Nagan, N.; Zhu, H.; Akmaev, V. R.; Zhou, Z.; Rohlfs, E. M.; Flynn, K.; Hendrickson, B. C.; Scholl, T.; Sirko-Osadsa, D. A.; Allitto, B. A. Pan-ethnic carrier screening and prenatal diagnosis for spinal muscular atrophy: clinical laboratory analysis of >72,400 specimens. *Eur. J. Hum. Genet.* **2012,** *20*, 27-32.

2. Kolb, S. J.; Kissel, J. T. Spinal muscular atrophy: a timely review. *Arch. Neurol.* **2011,** *68*, 979-984.

3. (a) Fallini, C.; Bassell, G. J.; Rossoll, W. Spinal muscular atrophy: The role of SMN in axonal mRNA regulation. *Brain Res.* **2012,** *1462*, 81-92; (b) Schrank, B.; Gotz, R.; Gunnersen, J. M.; Ure, J. M.; Toyka, K. V.; Smith, A. G.; Sendtner, M. Inactivation of the survival motor neuron gene, a candidate gene for human spinal muscular atrophy, leads to massive cell death in early mouse embryos. *Proc. Natl Acad. Sci. U S A* **1997,** *94*, 9920-9925; (c) Paushkin, S.; Gubitz, A. K.; Massenet, S.; Dreyfuss, G. The SMN complex, an assemblyosome of ribonucleoproteins. *Curr. Opin. Cell Biol.* **2002,** *14*, 305-312.

4. (a) Kolb, S. J.; Gubitz, A. K.; Olszewski, R. F., Jr.; Ottinger, E.; Sumner, C. J.; Fischbeck, K. H.; Dreyfuss, G. A novel cell immunoassay to measure survival of motor neurons protein in blood cells. *BMC Neurol.* **2006,** *6*, 6; (b) Crawford, T. O.; Paushkin, S. V.; Kobayashi, D. T.; Forrest, S. J.; Joyce, C. L.; Finkel, R. S.; Kaufmann, P.; Swoboda, K. J.; Tiziano, D.; Lomastro, R.; Li, R. H.; Trachtenberg, F. L.; Plasterer, T.; Chen, K. S. Evaluation of SMN protein, transcript, and copy number in the biomarkers for Spinal Muscular Atrophy (BforSMA) clinical study. *PLoS One* **2012,** *7*, e33572.

5. Kaczmarek, A.; Schneider, S.; Wirth, B.; Riessland, M. Investigational therapies for the treatment of spinal muscular atrophy. *Expert Opin. Invest. Drugs* **2015,** *24*, 867-881.

6. (a) Hua, Y.; Sahashi, K.; Rigo, F.; Hung, G.; Horev, G.; Bennett, C. F.; Krainer, A. R. Peripheral SMN restoration is essential for long-term rescue of a severe spinal muscular atrophy mouse model. *Nature (London, U. K.)* **2011,** *478*, 123-126; (b) Passini, M. A.; Bu, J.; Richards, A. M.; Kinnecom, C.; Sardi, S. P.; Stanek, L. M.; Hua, Y.; Rigo, F.; Matson, J.; Hung, G.; Kaye, E. M.; Shihabuddin, L. S.; Krainer, A. R.; Bennett, C. F.; Cheng, S. H. Antisense oligonucleotides delivered to the mouse CNS ameliorate symptoms of severe spinal muscular atrophy. *Sci. Transl. Med.* **2011,** *3*, 72ra18/1-72ra18/11; (c) Sahashi, K.; Ling, K. K. Y.; Hua, Y.;

Wilkinson, J. E.; Nomakuchi, T.; Rigo, F.; Hung, G.; Xu, D.; Jiang, Y.-P.; Lin, R. Z.; Ko, C.-P.; Bennett, C. F.; Krainer, A. R. Pathological impact of SMN2 mis-splicing in adult SMA mice. *EMBO Mol. Med.* **2013,** *5*, 1586-1601.

7. Naryshkin, N. A.; Weetall, M.; Dakka, A.; Narasimhan, J.; Zhao, X.; Feng, Z.; Ling, K. K. Y.; Karp, G. M.; Qi, H.; Woll, M. G.; Chen, G.; Zhang, N.; Gabbeta, V.; Vazirani, P.; Bhattacharyya, A.; Furia, B.; Risher, N.; Sheedy, J.; Kong, R.; Ma, J.; Turpoff, A.; Lee, C.-S.; Zhang, X.; Moon, Y.-C.; Trifillis, P.; Welch, E. M.; Colacino, J. M.; Babiak, J.; Almstead, N. G.; Peltz, S. W.; Eng, L. A.; Chen, K. S.; Mull, J. L.; Lynes, M. S.; Rubin, L. L.; Fontoura, P.; Santarelli, L.; Haehnke, D.; McCarthy, K. D.; Schmucki, R.; Ebeling, M.; Sivaramakrishnan, M.; Ko, C.-P.; Paushkin, S. V.; Ratni, H.; Gerlach, I.; Ghosh, A.; Metzger, F. SMN2 splicing modifiers improve motor function and longevity in mice with spinal muscular atrophy. *Science (Washington, DC, U. S.)* **2014,** *345*, 688-693.

8. Palacino, J.; Swalley, S. E.; Song, C.; Cheung, A. K.; Shu, L.; Zhang, X.; Van Hoosear, M.; Shin, Y.; Chin, D. N.; Keller, C. G.; Beibel, M.; Renaud, N. A.; Smith, T. M.; Salcius, M.; Shi, X.; Hild, M.; Servais, R.; Jain, M.; Deng, L.; Bullock, C.; McLellan, M.; Schuierer, S.; Murphy, L.; Blommers, M. J. J.; Blaustein, C.; Berenshteyn, F.; Lacoste, A.; Thomas, J. R.; Roma, G.; Michaud, G. A.; Tseng, B. S.; Porter, J. A.; Myer, V. E.; Tallarico, J. A.; Hamann, L. G.; Curtis, D.; Fishman, M. C.; Dietrich, W. F.; Dales, N. A.; Sivasankaran, R. SMN2 splice modulators enhance U1-pre-mRNA association and rescue SMA mice. *Nat. Chem. Biol.* **2015,** *11*, 511-517.

9. (a) Woll, M. G.; Chen, G.; Choi, S.; Dakka, A.; Huang, S.; Karp, G. M.; Lee, C.-S.; Li, C.; Narasimhan, J.; Naryshkin, N.; Paushkin, S.; Qi, H.; Turpoff, A. A.; Weetall, M. L.; Welch, E.; Yang, T.; Zhang, N.; Zhang, X.; Zhao, X.; Pinard, E.; Ratni, H. Preparation of substituted

chromenones for treating spinal muscular atrophy. WO2013101974A1, 2013; (b) Lee, C.-S.; Choi, S.; Karp, G. M.; Koyama, H.; Ratni, H. Compounds for treating spinal muscular atrophy. WO2013130689A1, 2013.

10. Chen, G.; Dakka, A.; Karp, G. M.; Li, C.; Narasimhan, J.; Naryshkin, N.; Weetall, M. L.; Welch, E.; Zhao, X. Preparation of isochromenone derivatives for treating spinal muscular atrophy. WO2013112788A1, 2013.

11. Qi, H.; Choi, S.; Dakka, A.; Karp, G. M.; Narasimhan, J.; Naryshkin, N.; Turpoff, A. A.; Weetall, M. L.; Welch, E.; Woll, M. G.; Yang, T.; Zhang, N.; Zhang, X.; Zhao, X.; Green, L.; Pinard, E.; Ratni, H. Preparation of pyridopyrimidine derivatives and related compounds for treating spinal muscular atrophy. WO2013119916A2, 2013.

12. (a) Ringeissen, S.; Marrot, L.; Note, R.; Labarussiat, A.; Imbert, S.; Todorov, M.; Mekenyan, O.; Meunier, J.-R. Development of a mechanistic SAR model for the detection of phototoxic chemicals and use in an integrated testing strategy. *Toxicol. in Vitro* **2011,** *25*, 324-334; (b) Llano, J.; Raber, J.; Eriksson, L. A. Theoretical study of phototoxic reactions of psoralens. *J. Photochem. Photobiol., A* **2003,** *154*, 235-243.

13. Le, T. T.; Pham, L. T.; Butchbach, M. E. R.; Zhang, H. L.; Monani, U. R.; Coovert, D. D.; Gavrilina, T. O.; Xing, L.; Bassell, G. J.; Burghes, A. H. M. SMNDelta7, the major product of the centromeric survival motor neuron (SMN2) gene, extends survival in mice with spinal muscular atrophy and associates with full-length SMN. *Hum. Mol. Genet.* **2005,** *14*, 845-857.